The relative importance of wind and hydroclimate drivers in modulating ~~windblown~~ the interannual variability of dust emissions in Earth system models

Xinzhu Li[1], Longlei Li[2], Yan Feng[3], and Xin Xi[1]

[1]Department of Geological and Mining Engineering and Sciences, Michigan Technological University, Houghton, MI, USA
[2]Department of Earth and Atmospheric Sciences, Cornell University, Ithaca, NY, USA
[3]Environmental Science Division, Argonne National Laboratory, Lemont, IL, USA

Correspondence: Longlei Li (ll859@cornell.edu) and Xin Xi (xinxi@mtu.edu)

Abstract. Windblown dust emissions are ~~governed~~ controlled by near-surface wind speed and ~~soil~~ sediment erodibility, the latter ~~influenced by hydroclimate conditions and land use~~modulated by hydroclimate and land-use conditions. Accurate representations of ~~the influence of these drivers in Earth system models is~~ these drivers are critical for reproducing historical dust variability and projecting ~~dust responses to future climate and land-use changes . Here we evaluate the model consistency in simulating the interannual variability of dust emissions and quantify the variance explained by wind speed and hydroclimate drivers within~~ future dust changes in Earth system models (ESMs). This study examines the discrepancies among 21 ~~Earth system models and three climate zones (hyperarid, arid and semiarid) . In the hyperarid zone, the models exhibit~~ ESMs in the relative importance of wind speed versus five hydroclimate drivers in explaining the historical (1980–2014) variability of dust emissions from global drylands. In hyperarid areas, models show poor agreement in the simulated dust variability, with only ~~10~~9% out of 210 ~~pairwise comparisons showing~~ inter-model comparisons exhibiting significant positive correlations. In contrast, arid and semiarid ~~zones, the models display a dipole~~ areas exhibit a dual pattern driven by a "double-edged sword" effect of land surface memory: models with coherent hydroclimate variability show ~~improved~~ better agreement, whereas those with divergent hydroclimate representations show ~~increased disagreement. Most models~~ larger disagreement. While the ESMs capture the dominant ~~influence~~ role of wind speed ~~on dust emissions~~ in hyperarid areas~~except GFDL-ESM4 and CESM2-CAM-Kok, which display large spatial variability and anomalously high sensitivity to soil moisture and precipitation, respectively. Incorporating the~~ , they diverge markedly in the relative contributions of wind and hydroclimate drivers in arid and semiarid areas. Replacing the Zender et al. (2003) dust scheme with the Kok et al. (2014) scheme in CESM and E3SM generally ~~amplifies the dust sensitivity to hydroclimate drivers and reduces the wind contribution to explained variance, e.g., from 56% to 46% for CESM and from 86% to 75% for E3SM in the arid zone. These findings~~ strengthens hydroclimate influences while reducing wind speed contributions to simulated dust variability. MERRA-2 reanalysis produces stronger wind influences than most ESMs over global drylands. These results underscore the need ~~to improve the representations of near-surface winds~~ for improved low-level wind simulations in hyperarid areas and ~~hydroclimate and land surface processes~~ more realistic land surface and hydroclimate representations in arid and semiarid areas to reduce ~~model uncertainties in dust emission estimates~~uncertainties in global dust emission simulations.

1 Introduction

Windblown dust ~~aerosol is an essential element of the Earth's biogeochemical cycle, but has become a global concern due to its wide-ranging impacts on the climate, ecosystems, agriculture, and society. Dust~~ emission is modulated by ~~a number of atmospheric and land surface variables which can be grouped into three broad drivers: sediment supply , sediment availability, and wind erosivity~~near-surface wind speed and the supply and erodibility of fine-grain sediments, which collectively determine the timing, location, duration, ~~intensity, and impacts~~ and intensity of dust events~~(?)~~. The most abundant ~~*sediment supply*~~ sediment supply is typically found in ~~low relief areas~~ low-relief regions with thick layers of ~~fine, unconsolidated materials generated via~~ unconsolidated materials produced by weathering, fluvial, and/or aeolian processes ~~(?). The *sediment availability* for airborne dust production is strongly affected by~~ (Bullard and Livingstone, 2002; Bullard et al., 2011). The erodibility of these fine materials depends on environmental conditions such as surface soil moisture and ~~surface~~ armoring (e.g., vegetation, soil ~~crust, non-erodible coarse particles~~crusts) which determine the minimum or ~~*threshold wind velocity* required to initiate dust mobilization (?). To initiate dust emission, near-surface winds must be strong enough to exceed the~~ threshold wind velocity ~~. As a result, the *wind erosivity* is dominated by infrequent, high wind events which generate sufficient drag to mobilize soil particles via saltation and sandblasting mechanisms. Depending on the relative importance of the three drivers, dust emission may fall into one of three distinct regimes: *supply-limited*, where a lack of suitable-sized sediments restricts dust emission ; *availability-limited*, where fine sediments are present but protected against erosion; and *transport capacity-limited*, where sediments are dry and exposed but near-surface winds are too weak to mobilize the particles.~~

~~The three dust emission drivers have been incorporated in global aerosol-climate models and Earth system models (ESMs) to capture the environmental controls on the~~ that must be reached to initiate the saltation-sandblasting process (e.g., Zender and Kwon, 2005; S . The environmental controls of dust ~~cycle. Dust emission schemes in many ESMs use a time-invariant dust source function~~ emission have been incorporated into Earth system models (ESMs) via parameterizations of dust emission fluxes as a function of various atmospheric, land surface, and soil parameters, many of which are interactively determined within the models. For example, the horizontal saltation dust flux is calculated as a function of the third or fourth power of wind velocity, reflecting the dominant role of infrequent, high-wind events in dust production (e.g., Owen, 1964; Bagnold, 1974; White, 1979; Kok et al., 2012) . Early parameterizations in ESMs use static dust source functions to represent the spatially varying sediment supply, with ~~high values generally associated with topographic depressions containing abundant alluvial or lacustrine deposits (???). These areas are generally assumed to have an unlimited sediment supply,~~ large values associated with low-relief regions where elevated dust burden has been frequently detected by satellite observations (e.g., Ginoux et al., 2001; Prospero et al., 2002; Zender et al., 2003) . The sediment supply is typically assumed to be unlimited in ESMs without accounting for depletion or replenishment over time~~(?). The sediment availability is strongly coupled with the hydroclimate variability~~ . In addition, the sediment erodibility is closely connected with hydroclimate and land surface processes in ESMs. ~~Specifically, a bare soil fraction scaling factor is~~ For example, surface soil moisture, which is simulated by the land model component, is often used to ~~exclude non-erodible surfaces~~ account for increases in erosion thresholds due to enhanced soil particle cohesion under wet conditions (Fécan et al., 1999). Many ESMs also use the bare soil fraction to adjust dust emissions from areas partially covered by snow, ice, or vegetation. Veg-

etation also ~~increases~~ acts to increase the aerodynamic surface roughness and ~~reduces the wind stress acting~~ reduce the available wind shear stress exerting on erodible surfaces, which can be represented by ~~a drag partitioning scheme (??). In addition, ESMs incorporate the role of soil moisture in enhancing the threshold wind velocity or suppressing dust emissions if the soil water content exceeds a given threshold (e.g., ?). Finally, ESMs parameterize the horizontal dust flux as the third or fourth power of wind speed once the threshold wind velocity is reached. This nonlinear relationship, combined with the skewed distribution of wind speeds, reflect the dominant contributions of rare, high-wind events to global dust emissions (??). Representing dust-producing wind events in ESMs remains a major challenge, since peak-wind generation mechanisms (such as convective downdrafts) often occur at spatial scales smaller than the typical grid spacing of ESMs (????).~~ drag partitioning schemes but this effect is currently not considered in most ESMs (Raupach et al., 1993; Marticorena and Bergametti, 1995; Shao, 2001).

~~The~~ Numerous studies have evaluated the consistency and performance of current ESMs in simulating the global dust cycle under the Aerosol Comparisons between Observations and Models (AeroCom) initiative and Coupled Model Intercomparison Project (CMIP) ~~have facilitated the intercomparison of ESMs in simulating the global dust cycle (????????). Generally, the~~ (Textor et al., 2006; Huneeus et al., 2011; Kim et al., 2014; Wu et al., 2020; Gliß et al., 2021; Zhao et al., 2022; Kim et al., 2024). Overall, these studies suggest that modern-day dust aerosol column burden is reasonably constrained by ground- and satellite-based aerosol optical depth (AOD) ~~observations over continental outflow areas, resulting in better model agreement compared to~~ retrievals, leading to better inter-model agreement than those in dust emission and deposition estimates. ~~? suggested that model tunings~~ Knippertz and Todd (2012) pointed out that model tuning to match satellite observations, e.g., via the use of dust source functions, ~~induce~~ induces a compensational effect between dust emission and deposition, both of which lack direct observational constraints at ~~global scales~~the global scale. Indeed, previous AeroCom and CMIP model intercomparisons ~~consistently show large discrepancies in the global total and regional distribution of dust emissions (????). While most ESMs roughly capture the annual cycle of dust over major source regions, they struggle in reproducing the dust interannual variability and relationships with wind speed and soil bareness (????). Recent studies suggested that all CMIP models~~ reported substantial discrepancies in global dust emission estimates, with differences spanning an order of magnitude, as well as persistent difficulties in reproducing historical dust variability and its relationships with key driving factors (Huneeus et al., 2011; Evan et al., Kok et al. (2023) further suggested that current ESMs failed to capture the ~~large~~ increase of global dust burden since preindustrial times, likely due to inaccurate model representations of ~~historical~~ the climate and land-use ~~changes~~ drivers of dust emissions, and/or the dust sensitivity to ~~these changes ??. Together, these studies underscore the persistent uncertainties and limited predictive capability of ESMs in simulating the response of windblown dust emissions to hydroclimate variability and land surface changes.~~ driving factors.

The model discrepancies can be ~~explained, at least in part,~~ partly explained by the choice of dust emission schemes. ~~Earlier-generation schemes relied on empirical, temporally-invariant~~ Earlier schemes rely on static dust source functions to shift emissions towards satellite-observed ~~hotspot regions (??)~~hot spot regions (e.g., Ginoux et al., 2001; Zender et al., 2003), whereas newer ~~schemes adopt more mechanistic approaches that account for sediment availability as a function of land surface conditions, thereby eliminating the need for dust source functions (?). These process-based schemes also introduce more realistic parameterizations of sandblasting efficiencyto represent the momentum transfer from salting soil grains to~~

~~the entrainment of fine particles into the atmosphere (??). With improved model physics, process-based schemes usually involve more extensive input parameters with greater uncertainties~~parameterizations replace prescribed dust source functions with more explicit formulations of sediment erodibility that increase the dust emission sensitivity to soil-moisture-dependent erosion thresholds (e.g., Kok et al., 2014b; Leung et al., 2023). Dust schemes also differ in how they represent the sandblasting efficiency, defined as the ratio of the vertical dust flux to the saltation flux: some schemes assume a global constant (e.g., Ginoux et al., 2001; , whereas more sophisticated schemes account for the dependence of sandblasting efficiency on soil properties and wind speed (e.g., Zender et al., 2003; Kok et al., 2014b). The choice of wind speed also varies: ~~some~~ while some dust schemes use 10-m ~~wind speeds for simplicity, while~~ winds, others use friction velocity ~~, which better captures the wind~~ which more accurately represents the wind shear stress acting on ~~soil~~ erodible surfaces but requires ~~information on surface roughness . Because surface roughness lengthis poorly constrained by observations, models employ varying assumptions and tunings to account for its effects on dust emission (e.g., ???).~~ specification of surface roughness length. In general, more sophisticated schemes, which are derived based on small-scale wind tunnel experiments, require more extensive input parameters which are often poorly constrained at climate model grid levels, necessitating assumptions and empirical tunings. For instance, due to limited data availability, surface aerodynamic roughness is often prescribed as a global constant or based on static satellite-derived maps (e.g., Peng et al., 2012; Tegen et al., 2019). ESM-simulated soil water content may lack the accuracy or dynamic range required by dust emission parameterizations. As a result, some models apply additional tunings or alternative treatments of soil moisture effects (e.g., Zender et al., 2003; Volodin and Kostrykin, 2016), while others disable the soil moisture dependence entirely (e.g., Noije et al., 2021; Shevliakova et al., 2024).

Even ~~with~~ when using the same dust emission scheme, ESMs can ~~diverge substantially~~ still diverge in dust emission simulations due to differences in model configurations (e.g., horizontal resolution, vertical levels), input datasets, parameter tunings, and coupled ~~parameterizations~~physical processes. For instance, the bare soil fraction is determined from land cover type, vegetation fraction, and snow~~areal~~ /ice area extent, all of which may differ ~~between ESMs. In particular, vegetation cover~~ across ESMs. Vegetation cover itself may be prescribed from ~~a fixed~~ satellite climatology or simulated interactively. ~~Further discrepancies may result from differences in~~ ESMs also differ in their representations of soil properties (e.g., hydraulic conductivity), soil column structure (e.g., number and thickness of layers), and ~~hydrologic processes~~ land surface hydrologic formulations (e.g., precipitation, runoff, evaporation), which ~~ultimately determine the water content of top soil layers and consequently the threshold wind velocity~~collectively determine the surface soil moisture needed by dust emission schemes. The soil moisture ~~effect on threshold wind velocity is also~~ effects may be treated inconsistently, e.g., in ~~calculating the residue~~ how models define the residue moisture level below which ~~soil moisture~~ dust emission is assumed to ~~have no effects on dust emission (e.g., ???)~~be independent on soil water content (e.g., Ginoux et al., 2001; Evans et al., 2016; Volodin and Kostrykin, 2016). Moreover, ESMs employ different ~~parameterizations for~~ planetary boundary layer and ~~subgrid processes, which affect the momentum transfer from the atmosphere to the surface. Because of the strong coupling between dust emission and boundary layer and land surface processes~~surface flux parameterizations, which influence the simulation of near-surface winds and extreme wind events pertinent to dust mobilization and transport. Given the inherent differences in dust process representations and the lack of direct observational constraints, it is thus not surprising that ~~dust emission estimates are strongly model-dependent~~ESM-simu

dust emission fluxes exhibit substantial discrepancies, as documented in previous AeroCom and CMIP intercomparison studies. Therefore, ESM-simulated dust emissions are best viewed as an unconstrained, model-specific quantity characterized by a dynamic range defined by the parameterizations, configurations, and parameter tunings of individual models, similar to Koster et al. (2009)'s view on root-zone soil moisture.

While ~~past studies have documented the large model diversity in the climatological dust cycle (e.g., ????), key questions remain as to whether current ESMs consistently capture the temporal variability of historical dust emissions and their sensitivities to wind and hydroclimate~~ model discrepancies in global dust emission estimates are well documented, a key remaining question is how consistently and accurately current ESMs represent the interannual variability of dust emission and its sensitivity to underlying physical drivers. Addressing ~~these questions~~ this question is essential for understanding and reducing model uncertainties in ~~projecting dust emission responses to future changes in climate and land use~~predicting dust responses to climate and land-use changes. In this study, we ~~provide a detailed assessment of~~ focus on the interannual variability ~~and physical drivers of dust emissions, by quantifying the inherent relative influence of near-surface wind speed and hydroclimate conditions in modulating the dust variability within~~ of ESM-simulated dust emissions from global drylands and apply a statistical framework to diagnose the physical controls of dust emissions. Based on fully-coupled historical simulations from a suite of ~~state-of-the-art ESMs . Compared to previous studies, we shift the focus from climatological means to temporal variability and move beyond documenting uncertainties to diagnosing their physical origins, thereby offering critical insights for improving the dust representation in ESMs.~~

~~A major challenge in evaluating dust models is the lack of direct, global observational constraints on dust emission fluxes. While~~ ESMs and two aerosol reanalysis products, we examine the extent of inter-model agreement in simulating the interannual dust variability across different climate aridity regimes and quantify the relative importance of a common set of physical drivers in explaining the simulated dust variability within individual models. Although satellite-derived dust ~~optical depth and long-term surface concentration records provide valuable insights into dust variability (e.g., ???)~~AOD and in-situ dust measurements provide valuable constraints on dust variability (e.g., Prospero and Lamb, 2003; Voss and Evan, 2020), they integrate ~~information from~~ the effects of emission, transport, and deposition, making it difficult to isolate the emission process ~~(the focus of this work). Therefore, rather than validating absolute model performance against observations~~itself. Also, due to lack of global validation data, we focus on diagnosing ~~the~~ inter-model ~~consistency of simulated dust emission variability. Here we treat model-simulated dust emission flux as an unobservable, model-specific quantity, which is characterized by a dynamic range defined by the internal model variability, parameterizations, parameter uncertainties, and model configurations. This approach is analogous to ?'s view of root-zone soil moisture and reflects the fact that model-simulated dust emission fluxes cannot be validated with field observations. While model-simulated dust emissions are essentially approximations of the true state they aim to reproduce, their true information content lie not necessarily in the absolute magnitudes but in their spatiotemporal variability and sensitivities to physical drivers. By quantifying the relative influence of wind speed and hydroclimate conditions over different climate regimes (i.e., hyperarid, arid and semiarid), this study provides new insights into model discrepancies and biases in dust emission representations~~inconsistency in representing the dust emission variability and its physical controls, rather than validating individual model performance against observations.

Table 1. Summary of ~~the~~ Earth system models and aerosol reanalysis datasets considered in this study. Dust source function (DSF) ~~column~~ indicates whether ~~an empirical~~ a static dust source function is used. Leaf area index (LAI) ~~column~~ indicates whether LAI is treated as a prognostic variable. D_m ~~,~~ is the dust particle diameter upper limit. u_* is friction velocity. u_{10} is 10-m wind velocity.

Model	Resolution	D_m	Wind	DSF	LAI	Dust Scheme	Refe
~~CESM2-CAM-Zender~~ CESM2-WACCM-Zender	0.9°×1.25°	10	u_*^3	Y	Y	~~?~~ Zender et al. (2003)	~~?~~ Ge
~~CESM2-WACCM-Zender~~CESM2-CAM-Zender	0.9°×1.25°	10	u_*^3	Y	Y	~~?~~ Zender et al. (2003)	~~?~~ All
CESM2-CAM-Kok	0.9°×1.25°	10	u_*^3	N	Y	~~?~~ Kok et al. (2014b)	~~?~~ Li
E3SM2-Zender	1°×1°	10	u_*^3	Y	~~Y~~ N	~~?~~ Zender et al. (2003)	~~?~~ Fer
E3SM3-Kok	1°×1°	10	u_*^3	N	Y	Kok et al. (2014b)	Xie e
CanESM5.0	2.8°×2.8°	-	u_*^3	Y	~~?~~ Y	~~?~~ Peng et al. (2012)	Swar
~~CanESM5-1~~ CanESM5.1	2.8°×2.8°	~~Bulk~~ -	u_*^3	Y	Y	~~?~~ Peng et al. (2012)	~~?~~ Sig
CNRM-ESM2.1	1.4°×1.4°	20	u_*^3	N	Y	~~?~~ Tegen et al. (2002)	~~?~~ Séf
EC-Earth3-AerChem	2°×3°	20	u_*^3	Y	N	~~?~~ Tegen et al. (2002)	~~?~~ No
GISS-E2.1-OMA	2°×2.5°	32	u_{10}^3	Y	N	~~?~~ Miller et al. (2006)	~~?~~ Mi
GISS-E2.1-MATRIX	2°×2.5°	32	u_{10}^3	Y	N	~~?~~ Miller et al. (2006)	~~?~~ Mi
GISS-E2.2-OMA	2°×2.5°	32	u_{10}^3	Y	N	~~?~~ Miller et al. (2006)	~~?~~ Rin
~~GFDL-ESM4 1°×1.25° 20 u_*^3 Y Y ? ?~~ HadGEM3-GC31	0.6°×0.8°	63	u_*^3	Y	N	~~?~~ Woodward (2011)	~~?~~ Ro
UKESM1.0	1.25°×1.9°	63	u_*^3	N	Y	~~?~~ Woodward (2001)	~~?~~ Wo
INM-CM5.0	1.5°×2°	~~Bulk~~ -	u_*^4	N	N	~~?~~ Volodin and Kostrykin (2016)	~~?~~ Vo
IPSL-CM6A-LR	1.26°×2.5°	~~Bulk~~ -	u_{10}^3	Y	Y	~~?~~ Balkanski et al. (2004)	~~?~~ Lu
MRI-ESM2.0	1.9°×1.9°	20	u_*^3	N	N	~~?~~ Shao et al. (1996)	~~?~~ Yu
MIROC6	1.4°×1.4°	10	u_{10}^3	N	Y	~~?~~ Takemura et al. (2009)	~~?~~ Tat
MIROC-ES2L	2.8°×2.8°	10	u_{10}^3	N	Y	~~?~~ Takemura et al. (2009)	~~?~~ Ha
MPI-ESM-1.2	1.9°×1.9°	~~Bulk~~ -	u_*^3	Y	Y	~~?~~ Tegen et al. (2019)	~~?~~ Ma
NorESM2	0.9°×1.25°	10	u_*^3	Y	N	~~?~~ Zender et al. (2003)	~~?~~ Sel
~~MERRA2~~ MERRA-2	0.5°×0.63°	20	u_{10}^3	Y	N	~~?~~ Ginoux et al. (2001)	~~?~~ Ra
JRAero	1.1°×1.1°	20	u_*^3	N	N	~~?~~ Shao et al. (1996)	~~?~~ Yu

The remainder of this paper is organized as follows. Section 2 describes the ESMs and ~~reanalysis datasets considered in this study,~~ aerosol reanalysis datasets and the dominance analysis technique~~used to quantify the joint and relative influence of dust emission drivers~~. Section 3 presents ~~the intercomparison of dust interannual variability~~ results on comparing model-simulated dust emission fluxes and the relative ~~influence~~ influences of wind speed ~~and hydroclimate conditions. The conclusions are summarized in Section 4.~~ versus hydroclimate drivers. Section 4 summarizes the main findings of this study.

2 Data and Approach

2.1 ESMs and aerosol reanalysis ~~products~~

~~Table 1 summarizes the ESMs and reanalysis products analyzed in this study, which differ in model resolution, vegetation process, and dust emission parameterizations, among other aspects. Among the 21 ESMs,~~ We consider a total of 21 ESMs as summarized in Table 1, including 18 ~~are~~ models from the CMIP6 ~~historical, fully-coupled experiments~~ fully coupled historical experiment (1980–2014). ~~We~~ For each model, we use the first ensemble member (r1i1p1f1) ~~from each model,~~ unless otherwise stated. ~~CMIP6 consists of several model families that share common heritage but differ in physics options and configurations. For instance, two Community Earth System Model (CESM) configurations employ the dust scheme of ?~~ Two CESM variants use the same dust emission scheme of Zender et al. (2003) (hereafter the Zender scheme) but ~~use different atmospheric schemes:~~ different atmospheric components: the Community Atmosphere Model (CESM2-CAM-Zender) ~~vs.~~ versus the Whole Atmosphere Community Climate Model (CESM2-WACCM-Zender)~~, with major differencesin the vertical extent and upper atmospheric processes.~~ . In addition, we conducted a CESM experiment (2004–2013) using the dust emission scheme of Kok et al. (2014b) (hereafter the Kok scheme; CESM2-CAM-Kok) (Li et al., 2022). We further conduct two E3SM model experiments (1980–2014) coupled with the Zender (E3SM2-Zender) and Kok (E3SM3-Kok) schemes, respectively (Feng et al., 2022; Xie et al., 2025). A key difference between the two schemes is that, the Zender scheme relies on a prescribed, time-invariant dust source function that shifts emissions towards contemporary dust source regions, whereas the Kok scheme applies more physically based parameterizations of soil erosion thresholds, thereby improving dust simulations without using prescribed dust source functions (Kok et al., 2014a). The paired CESM and E3SM experiments allow us to examine how the choice of dust emission schemes or host models affects the simulated dust variability and sensitivity to driving factors. Nonetheless, it is important to note that comparing these experiments is complicated by additional model differences. For example, CESM2-CAM-Zender does not account for dust mineralogy, whereas CESM2-CAM-Kok simulates dust as mineral components with observationally constrained mineral optical properties (Li et al., 2024). This may lead to inconsistent radiative feedback on meteorology and dust emissions. Similarly, E3SM3 incorporates extensive model updates relative to E3SM2, which may affect near-surface meteorological and land surface conditions relevant to dust emissions (Xie et al., 2025).

Several other model families share common heritage but differ in physics options and configurations. For example, CanESM5.1 incorporated physics and technical changes that improved mean climate and dust simulations relative to CanESM5.0 (Sigmond et al., 2023). Three GISS-E2 models use the same dust scheme ~~of ?~~ from Miller et al. (2006) but differ in model version (2.1 vs. 2.2) and aerosol microphysics ~~schemes~~scheme: One-Moment Aerosol (OMA; ensemble member r1i1p3f1) ~~vs.~~ versus Multiconfiguration Aerosol TRacker of mIXing state (MATRIX; ensemble member r1i1p5f1) ~~(??)~~(Rind et al., 2020; Miller et al., 2021). UKESM1.0 is ~~built upon~~ developed based on the HadGEM3-GC3.1 general circulation model~~, which~~ . They use the same dust scheme ~~of ? but differ in~~ from Woodward (2001) but employ different parameter tunings and dust source representations ~~(?). Similarly,~~ (Woodward et al., 2022). MIROC-ES2L ~~is based on~~ builds upon the MIROC general circulation model version 5.2 (MIROC5) ~~(?)~~(Hajima et al., 2020), while MIROC6 incorporates ~~updated physics which~~ physics updates that improved

the mean climate state and internal variability ~~relative~~ compared to MIROC5 ~~(?)~~(Tatebe et al., 2019). Both MIROC-ES2L and MIROC6 ~~adopt~~ use the dust scheme from the SPRINTARS ~~aerosol module (?)~~model (Takemura et al., 2009).

~~In addition to the CMIP6 archive, we consider an updated CESM (2004–2013) with the dust scheme of ? (hereafter the Kok scheme; CESM2-CAM-Kok) (?), and the Energy Exascale Earth System Model (E3SM, 1980–2014) using the Zender (E3SM2-Zender) and Kok (E3SM3-Kok) schemes (??). The key difference between the two schemes is that the Kok scheme adopts physically based soil erodibility parameterizations and eliminates the use of empirical dust source functions unlike the Zender scheme. These paired experiments allow us to evaluate how the choice of dust schemes (Zender vs. Kok) or models (CESM vs. E3SM) affect dust emission simulations. Nonetheless, we should point out that CESM2-CAM-Kok simulates dust as mineral components with observationally constrained mineral optical properties (?), whereas CESM2-CAM-Zender does not account for particle mineralogy and simulates different dust optical properties that may affect dust radiative feedback on meteorology. Also, E3SM3 includes extensive updates over E3SM2 that may affect the near-surface meteorological and land surface conditions relevant to dust emissions (?).~~

~~We further compare the ESMs~~ The ESMs are further compared with two aerosol reanalysis products with dust emission flux output: Modern-Era Retrospective Analysis for Research and Applications ~~version~~ Version 2 (~~MERRA2~~MERRA-2, 1980–2014) ~~(?)~~(Gelaro et al., 2017), and Japanese Reanalysis for Aerosol (JRAero, 2011–2017) ~~(?). MERRA2 is produced by the GEOS-5 data assimilation system with radiatively-coupled Goddard Chemistry Aerosol Radiation and Transport (GOCART) module.~~ (Yumimoto et al., 2017). Dust emission in ~~GOCART is represented using the ? scheme. JRAero is produced by the Japan Meteorological Agency MASINGAR mk-2 global aerosol transport model, which simulates dust emission using the ?~~ MERRA-2 is simulated using the Ginoux et al. (2001) parameterization within the GOCART aerosol module of GEOS-5 model. In JRAero, dust emission is simulated using the Shao et al. (1996) energy-based scheme ~~, same as~~ (same as in MRI-ESM2.0~~(??). The meteorological and land surface conditions in MERRA2 and JRAeroare constrained by observational data assimilation , and thus are expected to better capture historical climate and land cover changes than the ESMs. MERRA2 and JRAero also benefit~~) within the Japan Meteorological Agency MASINGAR mk-2 global aerosol transport model (Yumimoto et al., 2017; Y . In both MERRA-2 and JRAero, the meteorological inputs for dust emission calculations are constrained via data assimilation of in situ and remote sensing observations (including surface and upper-air wind measurements), which improves near-surface wind simulations compared to CMIP6 models (Gelaro et al., 2017; Yumimoto et al., 2017). The surface soil moisture in MERRA-2 also benefits from assimilation of observation-corrected precipitation. While both reanalyses assimilate bias-corrected total AOD ~~, which provides some constraint on the dust column burden but does not directly constrain dust emissions~~from satellites, the AOD assimilation is expected to have limited influence on dust emission simulations.

~~We evaluate the consistency between~~ To facilitate the comparison among ESMs and reanalysis products~~in representing the interannual variability of total dust emission fluxes. To facilitate comparison across common dust-emitting regions, we divide global dust source areas~~ , we classify global drylands into three climate ~~zones: hyperarid~~zones—hyperarid, arid, and ~~semiarid, based~~ semiarid—based on the aridity index (AI), defined as the ratio of ~~1970–2000~~ climatological mean precipitation to potential evapotranspiration ~~using the data from ?. The hyperarid~~ for 1970–2000 following (Zomer et al., 2022). Dry subhumid areas are not considered due to their negligible dust contributions. The hyperarid climate zone is defined as AI$\leq$0.05, arid

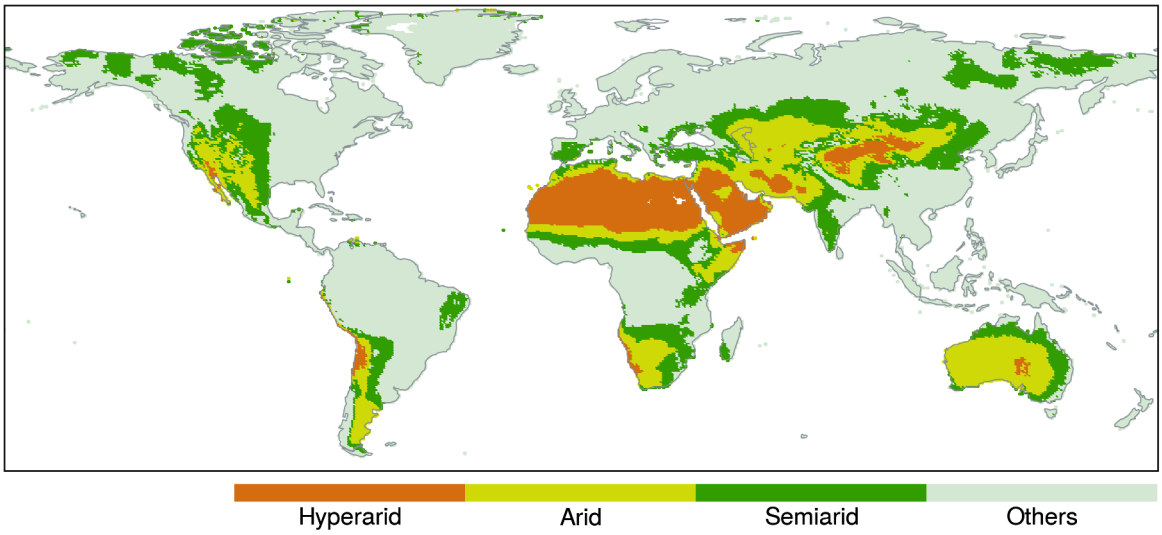

Figure 1. Definitions of ~~hyperarid, arid, and semiarid~~ climate aridity zones for model intercomparisons.

zone as 0.05<AI≤0.2, and semiarid zone as 0.2<AI≤0.5. ~~Using these climatologically defined zones allows us to assess model discrepancies over common dust-emitting areas. Figure 1shows that the hyperarid zone primarily covers~~ As shown in Fig. 1, hyperarid areas primarily cover North Africa, Arabian Peninsula, Iranian Plateau, and Tarim Basin. Arid and semiarid ~~zones~~ areas cover other major dust sources, including the Sahel (North Africa), Turan Depression (Central Asia), Gobi Desert (East Asia), Thar Desert (South Asia), Kalahari Desert (Southern Africa), Chihuahua Desert (North America), Patagonia steppe (South America), and the Great Sandy and Simpson Deserts (Australia). ~~The rationale of this climate zone-based analysis is that the relative importance of wind speed versus hydroclimate conditions is expected to depend strongly on climate regime. Specifically~~Generally, hyperarid areas are ~~expected to be~~ dominated by permanently dry, barren surfaces with ~~very~~ low hydroclimate variability, ~~and thus~~ such that dust emission is expected to be primarily controlled by wind speed. ~~Whereas, the~~ In contrast, arid and semiarid ~~zones are expected to exhibit increased~~ areas experience greater precipitation and hydroclimate ~~variability resulting in~~ fluctuations, which are expected to exert stronger influence on ~~the sediment availability~~sediment erodibility and dust emissions.

2.2 Dominance analysis technique

~~Past studies have~~ Previous studies commonly used linear regression coefficients to quantify ~~dust sensitivities~~ the dust sensitivity to its physical drivers ~~(e.g., ???)~~(e.g., Pu and Ginoux, 2016; Aryal and Evans, 2021; Zhao et al., 2022). In multiple linear regression, a regression coefficient represents the mean change in the response variable ~~per~~ (e.g., dust emission flux or AOD) associated with a unit change in a given predictor, while holding all other predictors constant. This interpretation assumes mutual independence among predictors, an assumption that is often violated by strong correlations among ~~hydroclimate variables.~~

~~As a result~~dust emission drivers. Consequently, linear regression coefficients ~~may yield~~ can cause misleading inference of ~~predictor importance . Moreover~~the relative importance of predictors. In addition, regression coefficients, standardized or not, may not provide a ~~direct comparison of predictor influence due to the varying dynamic rangesin ESMs~~consistent basis for comparing predictor importance across different ESMs, due to their inconsistent dynamic ranges.

In this study, we ~~apply~~ use the dominance analysis technique to quantify the relative ~~influence of wind and hydroclimate drivers on dust variability. Dominance analysis quantifies the marginal contribution of each predictor to the total explained variance (R^2) in the response variable by evaluating all possible subset models ($2^p - 1$ subsets for p predictors) in a multiple linear regression framework (**??**). For each predictor, the method calculates its average incremental contribution to the total R^2 across all subset models of the same size (i.e., models with the same number of predictors), and then average these values to obtain the predictor's unique contribution to the total R^2. A key property of this method is that the sum of individual predictor contributions equals the R^2 of the full model (i.e., with all predictors included), thereby allowing the partitioning of explained variance among correlated predictors. The predictor-specific R^2 values can thus be interpreted as the portions of total variance in the response variable that are uniquely and jointly attributed to each predictor, accounting for their interactions and multicollinearity.~~

~~We use the monthly~~ importance of multiple correlated predictors in explaining the variability of monthly total dust emission fluxes simulated by individual ESMs and the MERRA-2 reanalysis. JRAero is excluded from this analysis due to missing predictor data. Although the ESMs differ in how they partition total emissions into discrete size modes or bins, the size partitioning has minor effects on diagnosing the emission process itself. The predictors considered here operate upstream of the size partitioning, and control the initiation and magnitude of total dust emission ~~flux as the response variable and consider six predictors~~rather than its size-resolved characteristics. Here we consider a common set of six predictors from each model: 10-m wind speed, total precipitation (including liquid and solid phases), water content in the uppermost soil layer~~(hereafter as soil moisture)~~, 2-m specific humidity, 2-m air temperature, and leaf area index (LAI). ~~The total dust emission flux is a bulk quantity that represents the source strength. Although ESMs differ in how they partition the total flux into discrete particle size bins—a key factor influencing dust transport and atmospheric lifetime—we expect the size partitioning to have minimal impact on diagnosing the emission process itself, particularly its sensitivity to the selected predictors. The primary drivers of emission variability operate upstream of the size partitioning of mobilized soil particles. The six predictors are chosen because they are~~ Among them, 10-m wind speed represents the wind shear stress driving dust mobilization, while the remaining variables collectively represent the hydroclimate controls on sediment erodibility. The selected predictors are either directly used ~~as input parameters in dust flux calculations~~ in dust emission parameterizations or strongly correlated with dust emission intensity, as ~~suggested~~ shown in numerous studies ~~(e.g., **?????????**). Among them, wind speed represents the wind erosivity driver, while the remaining variables collectively represent the hydroclimate effect on sediment availability~~(e.g., Engelstaedter et al., 2003; Ravi et al., 2006; Zou and Zhai, 2004; Cowie et al., 2015; Kim and Choi, 2015; Xi and Sokoli
. Note that we donot not include all the physical drivers represented in each model because of limited data availability in the CMIP6 online archive, and because some models incorporate additional drivers not used by others. Hence we focus on a

common set of six readily available predictors to provide a consistent and fair comparison across the ESMs and MERRA-2 reanalysis.

Dominance analysis is ~~performed for all ESMs and MERRA2~~ applied to the ESMs and MERRA-2 over grid cells with nonzero ~~emissions using deseasonalized and normalized data. JRAero is excluded from the dominance analysis due to missing predictors and its short time span. We first subtract~~ dust emissions. The dust emission fluxes and predictors are first deseasonalized by subtracting month-wise climatological means ~~from the monthly dust fluxes and predictors, and then convert the deseasonalized data into~~ and then normalized to 0–1 range via min-max ~~normalization. For ESMs that use bare soil fraction as a scalingfactor in dust flux calculations (e.g., CNRM-ESM2.1, INM-CM5.0, UKESM1.0), the dust flux is first normalized by the bare soil fraction in order to isolate the influence of the selected predictors . The~~ scaling. Dominance analysis quantifies the marginal contribution of each predictor to the total explained variance (R^2) by evaluating all possible subset models ($2^p - 1$ subsets for p predictors) in a multiple linear regression framework (Budescu, 1993; Azen and Budescu, 2003). The approach first calculates the average incremental contribution of each predictor to the total R^2 across all subset models of the same size (i.e., models with the same number of predictors). These incremental R^2 values are then averaged to obtain the predictor's overall contribution to the total R^2. A key feature of this approach is that the sum of individual predictor contributions equals the total R^2 of the full model (i.e., with all predictors included), thereby allowing the partitioning of total explained variance among correlated predictors. The resulting grid-level ~~total and predictor-specific~~ predictor R^2 values from the ESMs and MERRA-2 are used to assess the ~~internal spatial variability (i.e., within each climate zone) and~~ spatial variability of predictor influences over different climate zones within each model, and the inter-model consistency in ~~the total explained variance and predictor relative importance~~ representing the relative importance of wind speed versus hydroclimate drivers.

3 Results

3.1 Climatological distribution

Figure 2 displays the climatological mean annual dust ~~fluxes from~~ emission fluxes from the 21 ESMs, ~~the model~~ their ensemble mean, and ~~MERRA2 and JRAero datasets for the~~ the MERRA-2 and JRAero reanalyses during 2005–2014 ~~period~~ (2004–2013 for CESM2-CAM-Kok and 2011–2017 for JRAero). All datasets capture the global dust belt stretching from West Africa across the Middle East to East Asia, as well as ~~the less intense~~ weaker sources in the Americas and Australia. Among the ESMs, E3SM3-Kok and HadGEM2-GC31 simulate the most extensive dust-emitting areas ~~including~~ extending to high-latitude and subhumid areas. ~~In contrast,~~ CESM2-CAM-Zender, CESM2-WACCM-Zender ~~,~~ and NorESM2 ~~simulate discrete and limited dust-emitting areas by excluding areas with~~ restrict emissions to regions where the dust source function ~~values below~~ exceeds 0.1~~.~~, resulting in discrete and spatially limited emission patterns. Conversely, E3SM2-Zender ~~uses the original , unmodified ?~~ employs the original dust source function ~~and thus produces~~ of Zender et al. (2003), producing a more spatially continuous emission pattern (Fig. 2e).

~~The global total dust flux varies greatly among the ESMs~~ Global annual dust emissions simulated by the ESMs vary greatly, ranging from 890 to 7727 Tg yr^{-1} with nearly an order of magnitude difference (Fig. 2a–2u). The ~~model~~ ensemble mean

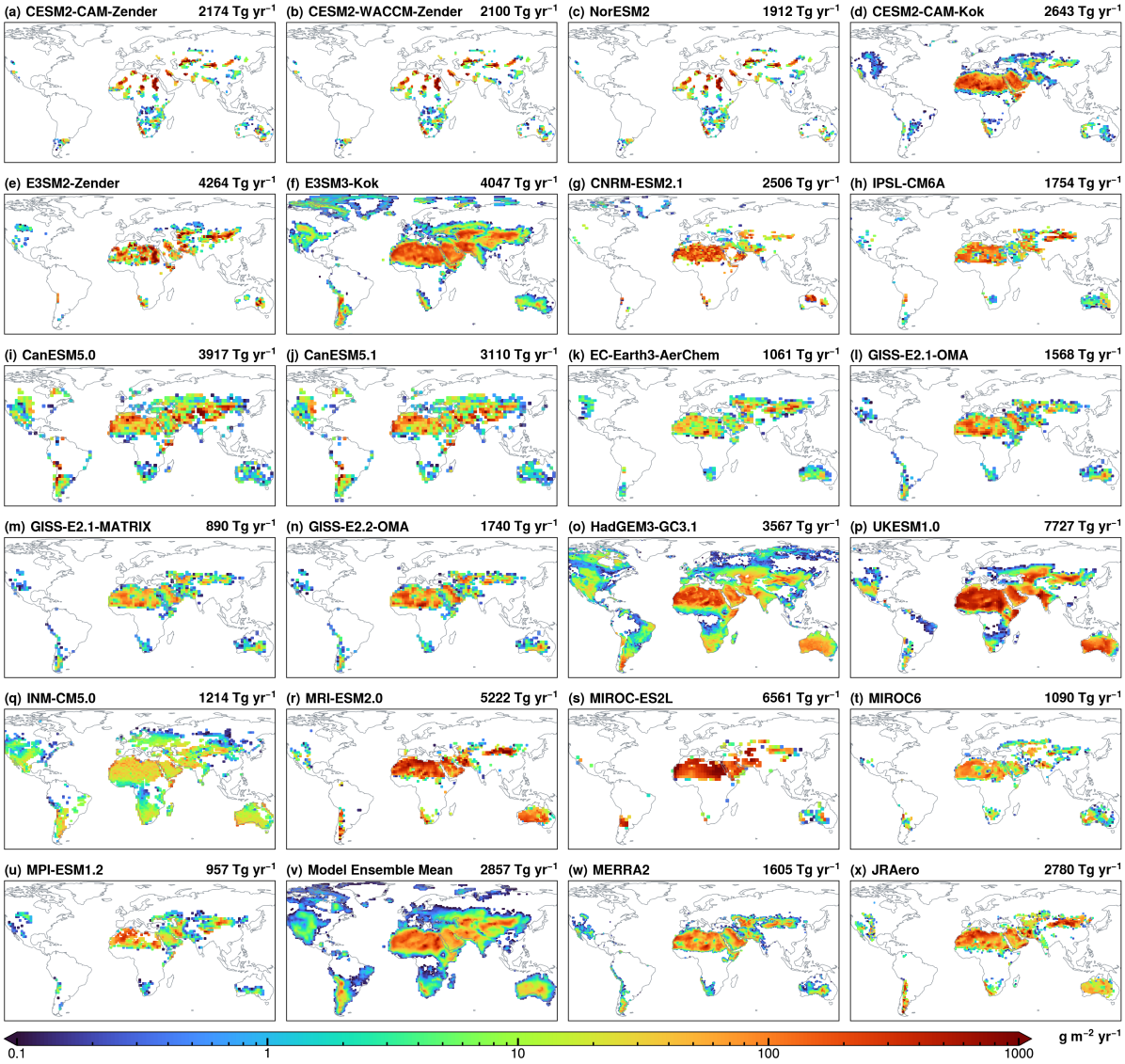

Figure 2. Climatological mean dust emission fluxes from (a–u) ~~individual~~ 21 Earth system models, (v) model ensemble mean, (w) ~~MERRA2~~ MERRA-2 reanalysis, and (x) JRAero reanalysis. Global annual total ~~dust~~ emissions are displayed on each panel.

estimate ~~is 2786 Tg yr^{-1}~~ (Fig. 2v) is 2857 Tg yr^{-1} with a standard deviation of ~~1821~~ 1835 Tg yr^{-1}, corresponding to a diversity of ~~65~~64% (defined as the ratio of standard deviation to ~~model~~ ensemble mean). Based on models with ~~a dust size upper~~ an upper particle size limit of 20 μm, global dust emissions vary from ~~1062~~ 1061 to 6561 Tg yr^{-1}, with a mean of ~~3012~~ 3048 Tg yr^{-1} and diversity of ~~51%. This uncertainty range is consistent with prior~~ 55%. The ensemble mean is close to JRAero (2780 Tg yr^{-1}, Fig. 2x), but considerably higher than MERRA-2 (1605 Tg yr^{-1}, Fig. 2w). Also, the ensemble mean exhibits a more spatially homogeneous pattern over North Africa and the Arabian Peninsula, whereas MERRA-2 and JRAero display more heterogeneous and localized emission patterns.

The model discrepancies in dust emission magnitude are consistent with previous assessments. For example, ~~?~~ Huneeus et al. (2011) compared 14 ~~models from~~ AeroCom Phase I models and reported a global dust emission range of 500–4400 Tg yr^{-1} ~~with a diversityof~~ (diversity=58%~~. Out of the 14 models, 7 models considered particle diameters up to~~), of which seven using a 20 ~~μm and reported a flux of~~ μm upper size limit yielded 980–4300 Tg yr^{-1} ~~with a diversityof~~ (diversity=46%). Similarly, ~~?~~ Gliß et al. (2021) compared 14 AeroCom Phase III models and ~~found~~ reported a range of 850–5650 Tg yr^{-1} with a diversity of 64%. ~~?~~ Based on 15 CMIP5 models, Wu et al. (2020) reported a range of 740–8200 Tg yr^{-1} ~~with a diversityof~~ (diversity=66%~~based on 15 CMIP5 models. Out of the 15 models, 7 models considering a diameter range of 0–20 μm yielded~~), with seven models using particle diameters up to 20 μm producing 740–3600 Tg yr^{-1} ~~with a diversityof~~ (diversity=43%). More recently, ~~? compared~~ Zhao et al. (2022) examined 15 ~~models from the~~ CMIP6 AMIP ~~experiment~~ models and reported a range of 1400–7600 Tg yr^{-1} with a diversity of 61%. ~~Past studies, together~~ Collectively, these studies, along with our results, ~~indicate persistent large~~ demonstrate persistent large model uncertainties in global dust ~~emissions, despite improvements~~ emission estimates despite advances in model resolutions and physics parameterizations, which reflects the unobservable, model-specific nature of dust emission fluxes.

~~The model ensemble mean global total dust flux is significantly higher than that of MERRA2 (1605 Tg yr^{-1}, Fig. 2w), but closely aligns with JRAero (2780 Tg yr^{-1}, Fig. 2x). In general, the model ensemble mean exhibits a more spatially homogeneous pattern over North Africa and Arabian Peninsula, whereas MERRA2 and JRAero display more heterogeneous and localized patterns.~~

Figure 3 displays the ~~fractional~~ contributions of different climate zones to global dust emissions. Based on the model ensemble mean, global dust emissions are partitioned as 61% from hyperarid, 27% from arid, and 5% from semiarid zones. In comparison, MERRA-2 and JRAero allocate the majority of dust emissions to hyperarid and arid zones, with negligible contributions from the semiarid zone.

The hyperarid zone accounts for more than half of global ~~total emissions in most ESMs except two models:~~ emissions in all ESMs except CanESM5.0, CanESM5.1, and INM-CM5.0~~, both of which~~ . These models simulate relatively uniform emission patterns with less than 50% from ~~the hyperarid zone (Fig. 2i, 2q). This may be due to known deficiencies of these two models~~hyperarid areas, possibly related to their dust emission parameterizations. As noted in ~~?, improper parameter tuning~~ Sigmond et al. (2023), parameter tunings related to the hybridization of dust tracers caused spurious dust events ~~and inaccurate dust distributions~~ in CanESM5.~~1~~.0. An interpolation error in the bare soil fraction also ~~distorted the model's dust source characterization, resulting in poor agreement with satellite observations (?).~~ contributed to dust simulation biases in

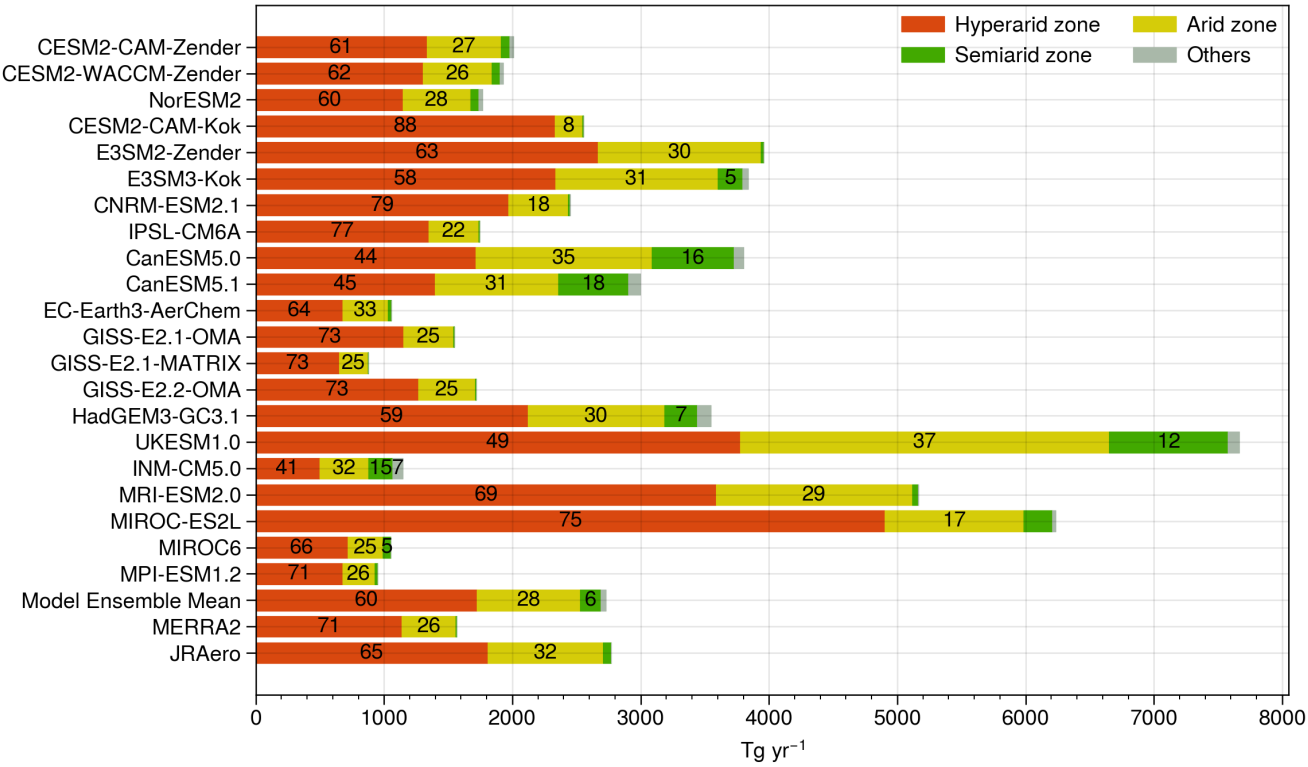

Figure 3. Contributions of different climate zones to global annual dust emissions. Numbers indicate percentages above 5%.

CanESM5.0 and CanESM5.1 compared to other CMIP6 models and satellite aerosol observations (Sigmond et al., 2023). The newer CanESM5.1 simulates 20% less dust globally but similar spatial distributions compared to CanESM5.0. In INM-CM5.0, the vertical dust flux is calculated as a function of ~~friction velocity only~~wind speed alone, without accounting for ~~the dependence of~~ land surface effects on the threshold wind velocity ~~on land surface conditions (??)~~(Volodin and Kostrykin, 2016; Volodin, 20 . While this simplification may be appropriate for ~~the hyperarid zone~~hyperarid areas, it can ~~introduce significant biases~~ overestimate emissions over arid and semiarid ~~zones where hydroclimate conditions play an increasingly important role in dust emissions~~areas where increased soil wetness and vegetation cover suppress dust mobilization.

~~Over the arid climate zone , the dust emission fraction ranges~~ Contributions of the arid zone range from 8% (CESM2-CAM-Kok) to 37% (UKESM-1.0), ~~reflecting substantial~~ indicating substantial model discrepancies compared to the hyperarid zone. The discrepancies ~~among the ESMs. These discrepancies~~ become even larger over the semiarid zone, where the ~~contribution~~ emission fraction ranges from less than 1% to 18%. ~~Three ESMs~~ Particularly, four models allocate more than 10% ~~of dust~~ to the semiarid zone: CanESM5.0 (16%), CanESM5.1 (18%), INM-CM5.0 (15%), and UKESM1.0 (12%). ~~Thus~~Overall, as the climate ~~zone shifts~~ regime transitions from hyperarid to semiarid, ~~the ESMs show larger discrepancies in their estimates of relative source strength. This climate zone-based comparison offers a first-order view of model representations of the~~ model-estimated

dust source strengths become less consistent, revealing increasing uncertainty in how ESMs represent dust sensitivity to hydroclimate conditions. ~~Based on the model ensemble mean, global dust emissions are partitioned as 61% from hyperarid, 27% from arid, and 5% from semiarid zones. In contrast, MERRA2 and JRAero produce most dust from hyperarid and arid zones, with negligible contributions from the semiarid zone.~~

Among the ESMs, CESM2-CAM-Zender ~~, CESM2-WACCM-Zender and NorESM2 produce similar~~ and CESM2-WACCM-Zender produce nearly identical total emissions and ~~regional fractions~~spatial patterns, suggesting that the choice between CAM and WACCM ~~has minimal influence when the same dust scheme (Zender) is used~~atmospheric components has minimal effect. The paired CESM and E3SM experiments~~show different changes in regional fractions. For instance, ~~, however, show opposite tendencies: contributions of the hyperarid zone ~~fraction increases~~ increase from 61% in CESM2-CAM-Zender to 88% in CESM2-CAM-Kok, but slightly ~~decreases~~ decrease from 63% in E3SM2-Zender to 58% in E3SM3-Kok. The GISS-E2 models ~~show no differences in the regional distributions . However, the total emission is~~ produce consistent distributions across different climate zones, although total emissions are about 40% lower when using the MATRIX aerosol scheme~~. This could be due to different model tuning parameters, or underestimation~~ , possibly due to parameter tunings or underrepresentation of coarse dust ~~particles (~~(diameter>5 μm~~diameter~~) in the MATRIX modal size distribution, as ~~pointed out by ?.~~ noted in Bauer et al. (2022).

UKESM1.0 ~~simulates~~ emits nearly twice as much dust as HadGEM3-GC3.1, ~~along with slightly more even~~ and exhibits slightly more uniform spatial distributions. As described in ~~?~~Woodward et al. (2022), UKESM1.0 is built ~~on~~ upon HadGEM3-GC3.1 but applies ~~model~~ parameter tunings that enhance friction velocity and suppress soil moisture~~. These tunings are expected to increase~~ , effectively increasing the wind gustiness and soil ~~dryness in~~ aridity, leading to more emissions in UKESM1~~.0, thereby strengthening dust emissions . UKESM1~~.0~~also excludes emissions from seasonally vegetated regions, resulting in smaller dust-emitting areas (Fig. 2p) compared to HadGEM3-GC3.1 (Fig. 2o).~~ . The three Japanese models (MRI-ESM2.0, MIROC-ES2L, and MIROC6) ~~exhibit large differences~~ also differ markedly in total emissions and, to a lesser ~~degree, regional~~ extent, spatial distributions. MRI-ESM2.0 produces similar regional fractions to JRAero but nearly ~~twice the total emissions~~doubles the total amount. Despite using the same dust ~~scheme~~parameterization, MIROC-ES2L ~~produces~~ emits roughly five times more dust than MIROC6. This discrepancy can be largely explained by ~~the~~ stronger winds in MIROC-ES2L, which produces 50% higher global mean wind speed than MIROC6. Moreover, MIROC6 prescribes non-zero LAI even in hyperarid ~~regions, which likely further suppresses dust emissions~~ areas, likely further suppressing dust generation relative to MIROC-ES2L (Hiroaki Tatebe, personal communications).

3.2 Interannual variability

This section ~~evaluates the consistency among the~~ examines the consistency of ESMs in simulating the interannual variability of dust emissions. Monthly dust emission fluxes from all ESMs are first regridded to a common resolution of 0.9°×1.25° (the native grid of CESM2). To remove the influence of annual cycles, ~~we subtract the~~ month-wise climatological means are subtracted from each grid cell ~~, yielding~~ to calculate deseasonalized dust emission flux anomalies. Spearman's rank correlation coefficients are then calculated between the ~~deseasonalized anomalies for all possible model pairs~~monthly anomalies for every

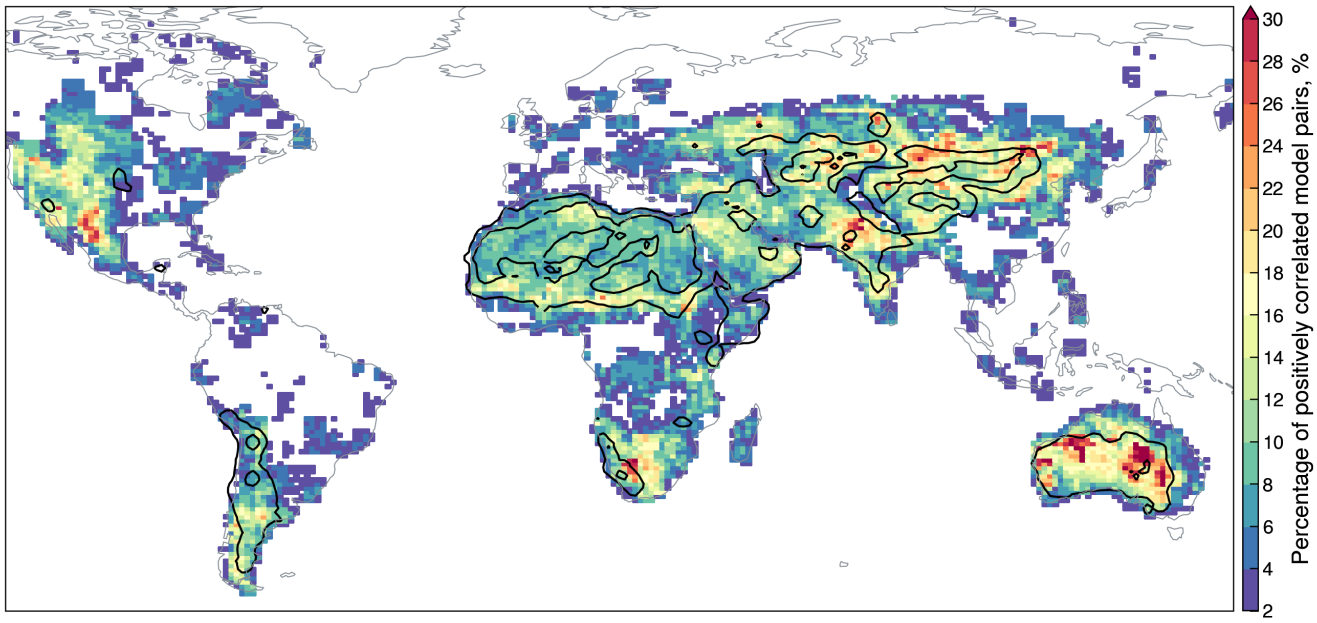

Figure 4. Percentage of statistically significant ($p \leq 0.1$), positive correlations out of ~~every possible~~ 210 pairwise comparisons of deseasonalized monthly dust emission fluxes from 21 Earth system models. Black contours ~~represent~~ indicate the model ensemble mean ~~annual dust~~ emission flux of 10 and 100 Tg yr^{-1}.

405 possible model pair. With 21 ESMs, this ~~yields~~ results in 210 pairwise comparisons. To quantify the ~~extent of inter-model~~ overall model agreement, we calculate the percentage of model pairs ~~that exhibit~~ exhibiting statistically significant ($p \leq 0.1$), positive correlations~~, which is displayed in Fig. 4.~~. A higher percentage indicates stronger ~~inter-model~~ model agreement in simulating the ~~interannual variability of dust emissions.~~ dust variability, and vice versa. The results are displayed in Fig. 4.

Despite its dominant ~~contributions~~ contribution to global dust emissions, the hyperarid zone ~~shows generally~~ exhibits poor
410 model agreement, with generally less than 10% of pairwise comparisons ~~yielding statistically significant~~, showing statistically significant positive correlations. Because dust emissions from hyperarid areas are ~~primarily controlled by~~ predominantly controlled by near-surface wind speed, this ~~weak~~ poor agreement reflects inconsistent wind simulations ~~in~~ among the ESMs. Indeed, we find that only 10% of model pairs produce ~~statistically significant, positively correlated wind variability in the hyperarid zone~~positively correlated monthly mean wind speed anomalies. Similarly, ~~?~~ Evan (2018) reported that dust-producing
415 winds over the Sahara ~~are mainly~~ Desert are driven by large-scale meteorological processes and that most CMIP5 models failed to capture the near-surface wind variability. These results suggest that ~~accurately representing~~ improving near-surface ~~winds is critical for reducing model discrepancies in dust~~ wind simulations can potentially reduce discrepancies in simulating the dust emission variability over hyperarid ~~areas~~regions.

~~Compared~~ In contrast to the hyperarid zone, arid and semiarid ~~zones (such~~ zones—such as the Sahel, South Asia, East ~~Asia~~
420 ~~and Australia) exhibit significantly stronger model~~ and Central Asia, Australia, and North America—exhibit significantly better

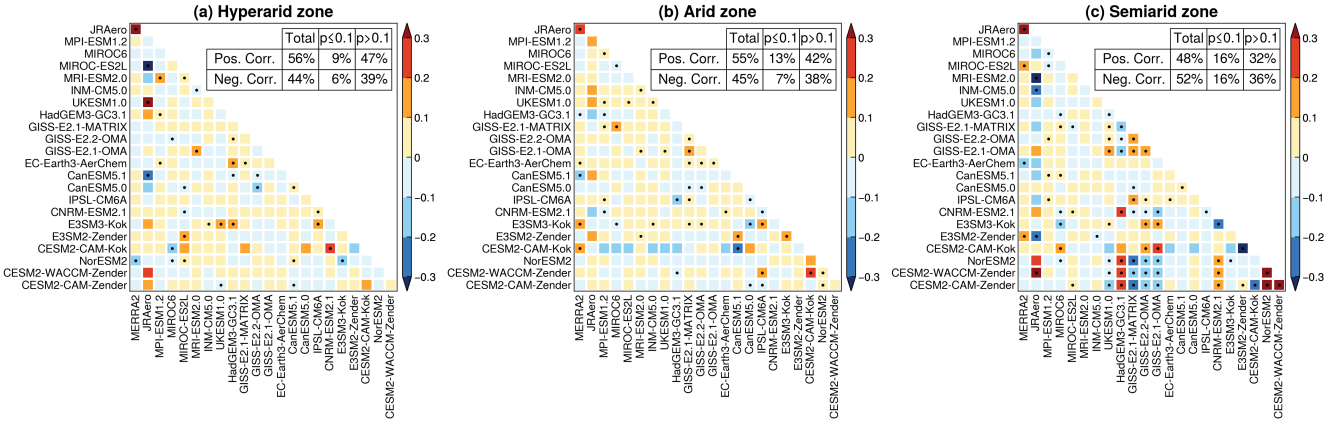

Figure 5. Spearman's rank correlation coefficients between dust emission flux anomalies averaged over hyperarid, arid, and semiarid climate zones. Dots indicate statistically significant correlations ($p \leq 0.1$). Summary tables are based on Earth system models only (~~MERRA2~~ MERRA-2 and JRAero not included).

agreement. To ~~illustrate~~ further assess how model consistency varies with ~~climate zones~~aridity, Fig. 5 presents ~~the~~ pairwise correlation matrices based on dust emission flux anomalies averaged over hyperarid, arid, and semiarid zones. The percentage of statistically significant, positively correlated model pairs increases from ~~10~~9% in the hyperarid zone to ~~14~~13% in the arid zone and ~~17~~16% in the semiarid zone~~, indicating progressively higher model agreement in regions where dust emissions are increasingly influenced by hydroclimate and land surface conditions~~. Meanwhile, the semiarid zone ~~exhibits~~ shows a larger percentage of negatively correlated model pairs (~~15%) compared to hyperarid (5~~16%) than the hyperarid (6%) and arid (~~6~~7%) zones. This ~~dipole~~ dual pattern suggests that as the climate regime transitions from hyperarid to semiarid, the ESMs exhibit both stronger agreement and ~~worsened~~ heightened disagreement in simulating ~~dust emission variability~~ the interannual variability of dust emissions.

~~What causes this complex behavior ? In~~ This behavior can be explained by the influence of antecedent land surface conditions on sediment erodibility in semiarid environment such as temperate grasslands and steppes ~~, dust emissions are strongly modulated by antecedent land surface conditions in addition to wind speed,~~ (Shinoda and Nandintsetseg, 2011; Nandintsetseg and Shinoda, . In these regions, factors such as precipitation, soil moisture, and vegetation ~~growth-decay cycle, which exert strong lagged influence on the soil erodibility(??)~~growth–decay cycles have lagged and long-lasting effects on sediment erodibility. For example, dry anomalies during the ~~prior wet season(e.g., reduced snowfall or rainfall~~ wet season, ~~accelerated snow retreat) can subsequently~~ such as reduced rainfall or earlier snowmelt, can reduce soil inter-particle cohesion and suppress vegetation growth, thereby prolonging bare soil exposure and increasing the wind erosion risk. This delayed ~~dust emission response to preceding drought exemplifies the effect of~~ response exemplifies the land surface memory ~~, whereby~~ effect, in which the slow adjustment of ~~land surface states (such as soil moisture, snow cover, and vegetation)~~ soil and vegetation conditions over weeks to months influences subsequent dust emission potentials long after the initial hydroclimate forcing (e.g., drought). Therefore,

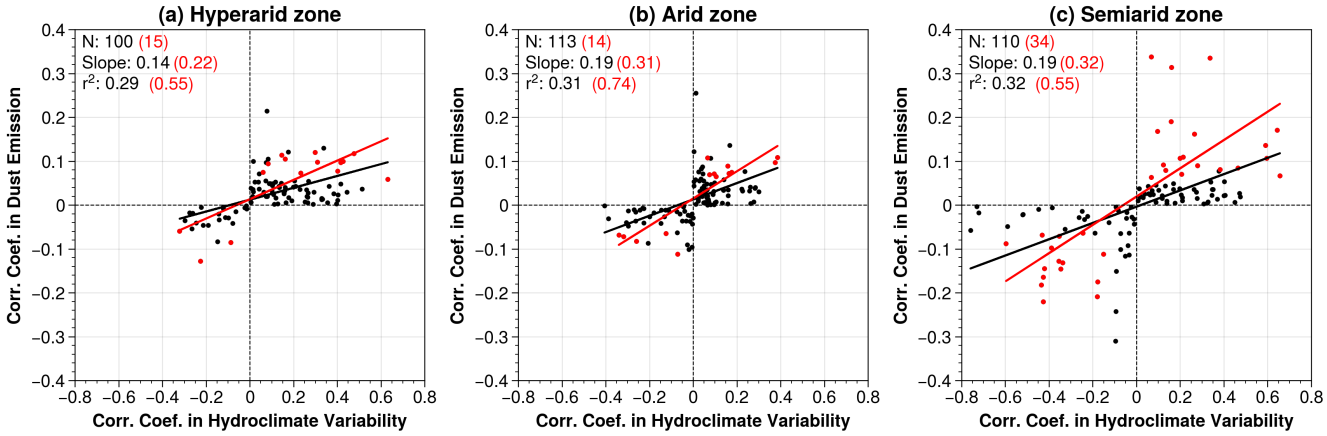

Figure 6. Statistical associations between pairwise model correlation coefficients ($p \leq 0.1$ shown in red) in dust emission fluxes and hydroclimate variability over (a) hyperarid, (b) arid, and (c) semiarid climate zones.

we ~~speculate~~ hypothesize that the simultaneous increase ~~of both model consistency and divergence~~ in both model agreement and disagreement from hyperarid to semiarid zones reflects a ~~"~~"double-edged sword~~"~~" effect of land surface memory: models with coherent representations of hydroclimate variability tend to converge in the simulated dust ~~emission~~ variability (i.e., more positive correlations), ~~while~~ whereas those with divergent hydroclimate representations diverge in the dust variability (i.e., more negative correlations).

~~Statistical associations between the pairwise model correlation coefficients ($p \leq 0.1$ shown in red) in dust emission fluxes and hydroclimate variability over (a) hyperarid, (b) arid, and (c) semiarid climate zones.~~

To verify this hypothesis, we examine the statistical association between pairwise model correlations in dust emissions and those in hydroclimate variability. Specifically, we ~~first perform a principle~~ perform a principal component analysis (PCA) of the five hydroclimate variables (i.e., precipitation, soil moisture, specific humidity, air temperature, LAI) separately for the hyperarid, arid, and semiarid zones. The leading ~~principle~~ principal component (PC1), which explains at least 40% of the total variance in all zones, is used as a proxy for the dominant hydroclimate variability. Spearman's rank correlation coefficients are then ~~calculated~~ computed for all pairwise ~~model~~ comparisons of deseasonalized monthly PC1 values, following the same approach as in Fig. 5.

Figure 6 compares the correlation coefficients for model pairs with the same sign (i.e., ~~either~~ both positive or both negative) in dust emission fluxes and hydroclimate PC1. The regression slope and coefficient of determination (r^2) quantify the degree of statistical association between ~~model~~ inter-model correlations in dust emission and hydroclimate variability. The positive ~~association in~~ relationships across all climate zones ~~suggests~~ suggest that ESMs with stronger consensus in hydroclimate variability also tend to produce more consistent dust variability~~, and vice versa~~. More importantly, ~~both~~ the number of significantly correlated model pairs (~~N~~N) and correlation strength (slope and r^2) show significant increases from hyperarid to semiarid zones. This ~~result~~ finding supports our hypothesis ~~regarding~~ on the dual role of land surface memory: it ~~enhances~~ tends to

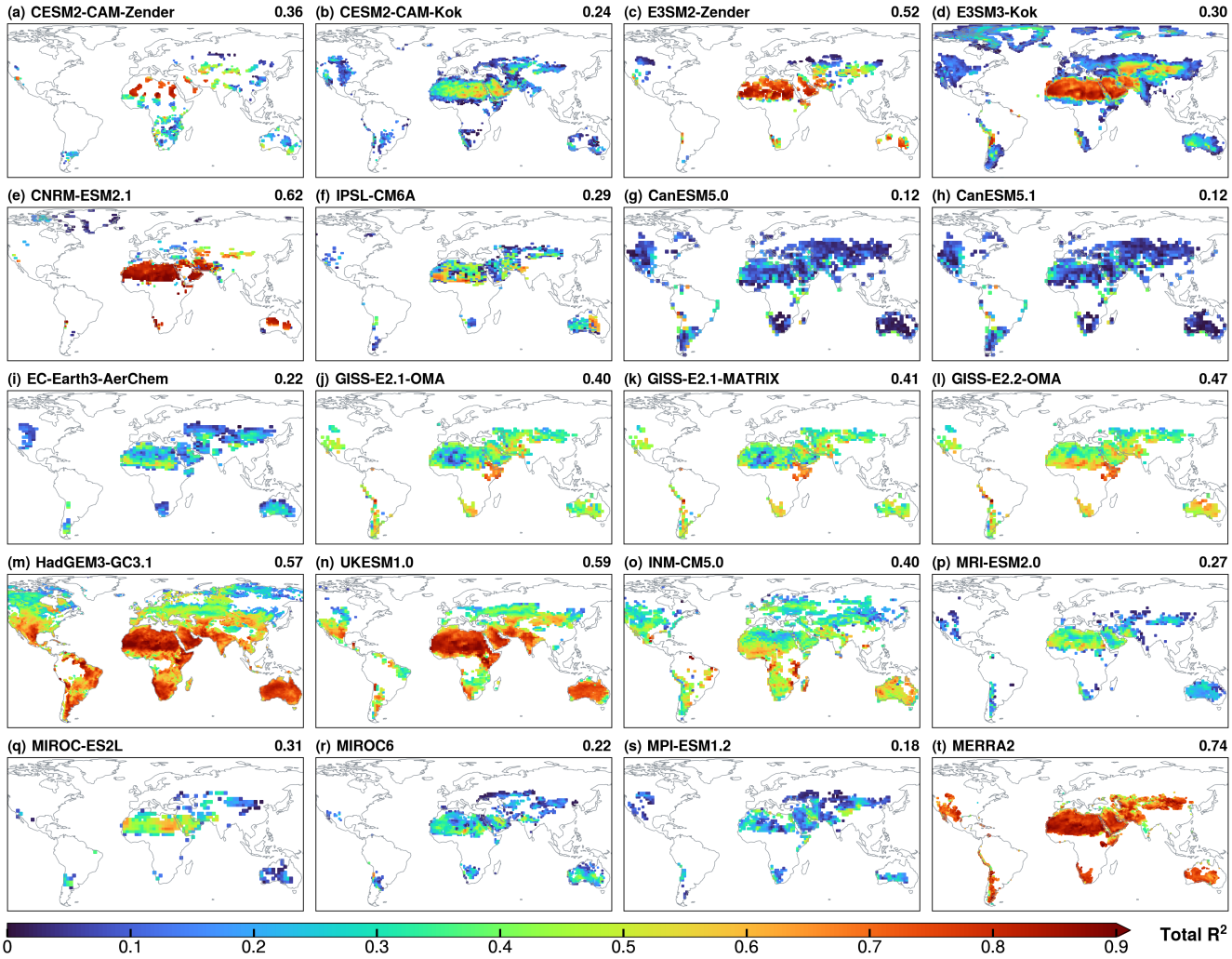

Figure 7. Total explained variance (R^2) in dust emission fluxes by six near-surface predictors (wind speed, precipitation, soil moisture, specific humidity, air temperature, and LAI) in Earth system models and ~~MERRA2~~MERRA-2. Global mean R^2 values are shown on each panel.

improve agreement among ESMs with coherent hydroclimate representations, while simultaneously ~~exacerbating~~ amplifying disagreement among those with divergent hydroclimate variability.

~~The ratio of wind speed-associated R^2 to the combined R^2 of five hydroclimate variables (precipitation, soil moisture, specific humidity, air temperature and LAI) in Earth system models and MERRA2.~~

3.3 Relative importance of wind speed versus hydroclimate drivers

3.4 ~~Relative importance of wind and hydroclimate drivers~~

In this section, we present ~~the dominance analysis of the collective and relative influence of wind~~ dominance analysis results on the joint and relative influences of wind speed and hydroclimate drivers on the ~~dust emission variability~~ simulated dust variability within individual ESMs. Figure 7 ~~presents the total variance explained (~~shows the total R^2 ~~) by near-surface wind speed and five hydroclimate variables (precipitation, soil moisture, specific humidity, air temperature, and LAI) in the ESMs and MERRA2~~by the selected six predictors. Results for CESM2-WACCM-Zender and NorESM2 are very similar to those ~~of~~ for CESM2-CAM-Zender and thus not shown.

~~The ESMs exhibit substantial differences~~ The ESMs show large discrepancies in the total R^2, reflecting ~~a large spread in the internal model variability and~~ inherent differences in the coupling strength between dust emission and the ~~six~~ selected predictors. ~~CanESM5.1 yields the lowest global~~ When ranked by the global mean R^2, CanESM5.0 and CanESM5.1 show the lowest explanatory power of the selected predictors, followed by MPI-ESM1.2, MIROC6, and EC-Earth3-AerChem~~, in which the selected predictors explain a relatively small fraction of the dust variability~~. The low ~~explanatory power may~~ total R^2 can be explained by several ~~reasons. Specifically, model deficiencies and errors (e.g., in CanESM5.1, Section~~ factors. We only consider six common predictors and may omit other predictors that are specific to some models (such as stem area index). Model biases (see Sect. 3.1) may weaken or distort the ~~relationships between dust emissions and the predictors. The use of over-simplified~~ relationship between dust emission and its physical drivers. Using simplified parameterizations and/or static land surface input ~~(e.g., in INM-CM5.0) may weaken the dust–predictor relationship~~can reduce the dust sensitivity to hydroclimate conditions. In addition, ~~dust emission involves inherently nonlinear processes and thus its relationship with~~ because dust emission is governed by highly nonlinear threshold processes, its dependence on the predictors may deviate from the ~~linearity assumption in~~ linear assumption underlying dominance analysis. As shown in Fig. 7, ~~the~~ total R^2 values ~~tend to be much~~ are generally lower in arid and semiarid ~~zones than in the hyperarid zone~~areas than in hyperarid areas, likely due to increased nonlinearity between dust emission and hydroclimate variables ~~which diminishes their collective explanatory power in a multilinear regressionframework. Finally, the use of monthly model output, due to data availability, may dampen the short-term variability and statistical association between dust emission and the predictors.~~ that diminishes the explanatory power of multilinear regression.

Despite these limitations, most ESMs produce significant total R^2 values~~over major source areas~~, especially in ~~the hyperarid zone where the total~~ hyperarid areas with R^2 ~~exceeds 0.6. Switching from the Zender to~~ generally above 0.5. Replacing the Zender with the Kok dust scheme ~~leads to generally lower~~ generally reduces the total R^2 ~~values in~~ in both CESM and E3SM (Fig. 7a–d). ~~The~~ GISS-E2 models show little differences between the OMA ~~or MATRIX~~ and MATRIX aerosol schemes, and a modest increase from version 2.1 to 2.2. UKESM1.0 and HadGEM3-GC3.1 show minimal differences, both ~~with~~ showing high R^2 values globally. MIROC6 yields lower R^2 than MIROC-ES2L, ~~especially over the hyperarid zone. MERRA2~~ particularly in hyperarid areas. MERRA-2 produces higher R^2 than most ESMs, especially ~~over~~ in arid and semiarid zones~~. In summary,~~

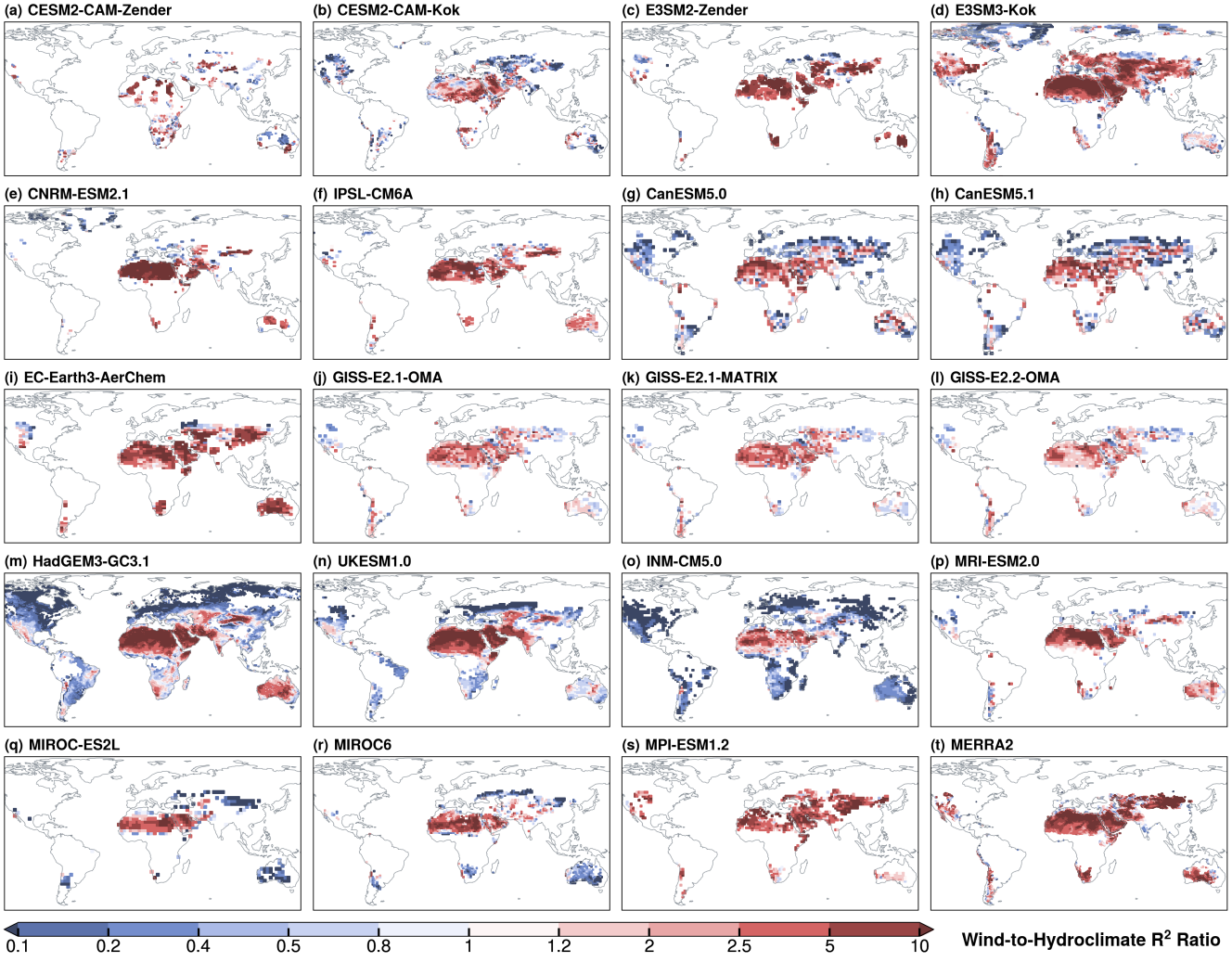

Figure 8. The ratio of wind-associated R^2 to the combined R^2 of five hydroclimate variables (precipitation, soil moisture, specific humidity, air temperature, and LAI) in Earth system models and MERRA-2.

~~there are large spatial variability within individual ESMs and large inter-model discrepancies in the variance explained by the~~ , indicating stronger coupling between dust emission and the selected predictors.

~~To assess the relative importance of wind and hydroclimate drivers, Fig. 8 displays~~

Figure 8 presents the ratio of ~~wind speed-associated~~ the wind-associated R^2 to the combined R^2 of five hydroclimate variables (precipitation, soil moisture, specific humidity, air temperature, and LAI). In all ESMs~~except GFDL-ESM4~~, the wind-to-hydroclimate R^2 ratio is well above 1 over ~~the hyperarid zone~~hyperarid areas, which is consistent with the ~~dominant role of~~ parameterization of vertical dust flux as a power-law function of wind speed in ~~controlling dust emissions from persistently~~

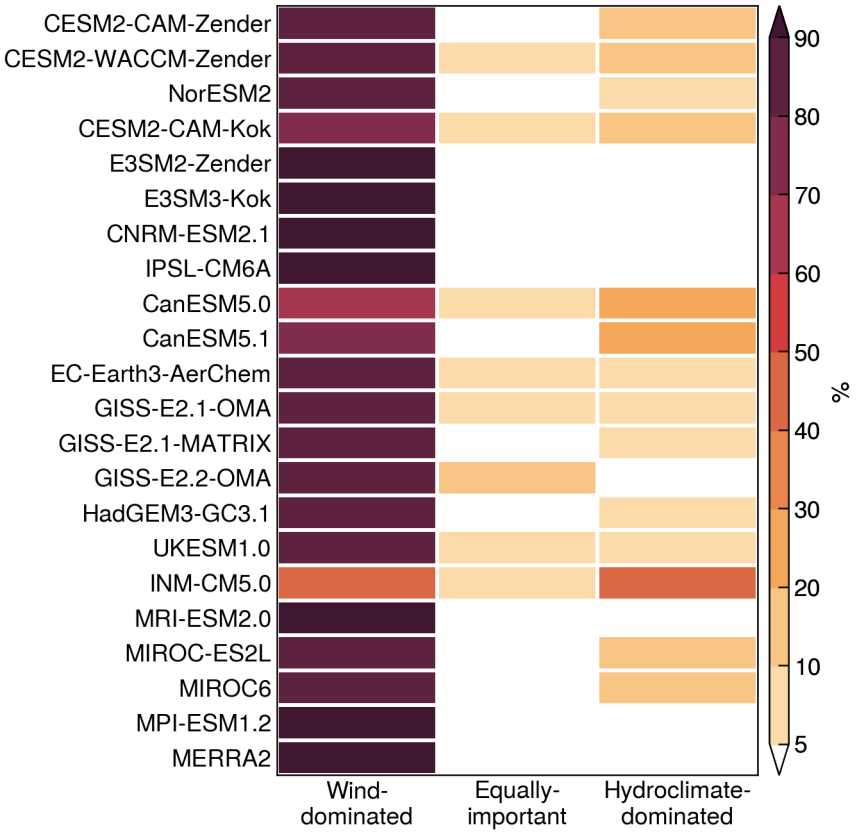

Figure 9. Fractional contributions of wind-dominated, equally-important, and hydroclimate-dominated regimes to global dust emissions in Earth system models and ~~MERRA2~~MERRA-2.

~~dry , barren surfaces~~ all models, and the expectation that dust emission from permanently dry and sparsely vegetated surfaces is primarily controlled by wind speed. In contrast, arid and semiarid ~~zones exhibit greater discrepancies~~areas exhibit much larger inconsistency, with ratios either above or below 1 depending on the model. This ~~reflects increased model discrepancies regarding~~ behavior may be due to inconsistent representations of hydroclimate controls on sediment erodibility, which in turn leads to disagreement in the relative importance of wind ~~and hydroclimate driversin transitional regions where~~ versus hydroclimate drivers. For example, most ESMs incorporate soil moisture as a correction to the erosion threshold velocity albeit using different formulations, while INM-CM5.0 treats soil moisture as a simple threshold above which dust emission is ~~increasingly influenced by hydroclimate and land surface conditions~~switched off. Such inconsistencies inevitably produce varying coupling strengths between dust emission and hydroclimate variables across models.

Based on the wind-to-hydroclimate R^2 ratios, we classify global dust-emitting areas into three regimes: wind-dominated (ratio$>$1.2), hydroclimate-dominated (ratio$<$0.8), and equally-important (0.8–1.2). ~~We then~~ Then we calculate the fractions of dust emissions ~~originating from the three regimes in~~ from these regimes within each model. The results are displayed in Fig.

9. The ESMs show general agreement in the "equally-important" regime, with most models ~~producing~~ simulating less than 10% ~~of dust~~ from regions where wind and hydroclimate drivers have nearly equal ~~influence on dust emissions. GFDL-ESM4 produces the highest contribution (12%) in this regime.~~ contributions.

The wind-dominated regime ~~contributes the majority of global dust emissions (>~~accounts for more than 80% ~~)~~ dust emissions in most ESMs~~and MERRA2~~, consistent with the dominant contribution of the hyperarid zone (Fig. 3). ~~However, three models yield anomalously low contributions: GFDL-ESM4 (36%),~~ Two models yield significantly lower estimates: INM-CM5.0 (~~54~~43%) and CanESM5~~.1 (75~~.0 (65%). ~~These deviations can be explained by different reasons.~~ As shown in Fig. 3, ~~INM-CM5.0 and CanESM5.1 produce relatively spatially homogeneous emission pattern, which explains the lower contributions from hyperarid or~~ these models simulate relatively homogeneous emission patterns, which consequently diminishes the relative contributions from wind-dominated ~~areas. In comparison, the low estimate in GFDL-ESM4 is due to the model's anomalously strong hydroclimate influence over the hyperarid zone. As shown in Fig. 8i, GFDL-ESM4 exhibits markedly low wind-to-hydroclimate ratios (<1) over North Africa, Arabian Peninsula, and Iranian Plateau, which are consequently misclassified into the hydroclimate-dominate regime. These regions are characterized by scarce precipitation and very low hydroclimate variability, which is expected to have negligible influence on dust emissions~~regions compared with other models. For CESM and E3SM, ~~switching from the Zender to~~ replacing the Zender with Kok dust scheme slightly reduces the wind-dominated dust fraction: from 85% to ~~80~~79% in CESM, and from 99% to 96% in E3SM. The three GISS-E2 models yield similar ~~estimates regardless of model version or aerosol scheme, with 82–85~~results, with 87–90% dust from the wind-dominated regime. ~~Similarly~~Likewise, UKESM1.0 and HadGEM3-GC3.1 yield ~~similar~~ nearly identical estimates, with 90% of dust ~~emitted~~ from wind-dominated regions. ~~MERRA2~~ MERRA-2 simulates 98% emissions from ~~the~~ wind-dominated ~~regime~~areas, higher than most ESMs. Three models produce significantly higher contributions from semiarid areas than others: CanESM5.0 (29%), CanESM5.1 (21%), and INM-CM5.0 (49%).

~~The above analysis not only confirms the anomalous dust emission patterns in CanESM5.1 and INM-CM5.0 as previously shown in Fig. 3, but also identifies GFDL-ESM4 as an outlier due to its misrepresentation of predictor relative importance . Here we further evaluate the contribution~~ To further assess the relative importance of wind speed versus hydroclimate drivers, we compute the fractional contributions of wind speed to the total R^2 ~~in different climate zones. For each climate zone, we use ridgeline plots to illustrate the~~ at each model grid cell. The statistical distributions of grid-level ~~wind speed-associated~~ wind-associated R^2 fractions ~~. The results~~ are displayed in Fig. 10. In ~~the ridgeline plots~~Fig. 10, if the median ~~value of wind speed-associated~~ wind-associated R^2 ~~fractions (denoted by a red vertical line in Fig. 10) is above~~ fraction exceeds 50%, it ~~means~~ indicates that wind speed dominates ~~the~~ dust variability at more than half of the grid cells ~~. If the median value is~~ within a climate zone. Conversely, if the median falls below 50%, ~~the dust variability is dominated by hydroclimate drivers at more than half of the~~ hydroclimate drivers exert dominant control over the majority of grid cells.

In the hyperarid zone (Fig. 10a), ~~most ESMs and MERRA2~~ the majority of ESMs capture the dominant ~~control of wind speed, with the median~~ wind control, with median wind-associated R^2 fractions exceeding 80%. The three GISS-E2 models ~~show similar spatial variability, with slightly lower median values (~70~~display slightly lower wind contributions (67–74%). ~~Two models stand out as notable outliers: GFDL-ESM4 and~~ In contrast, CESM2-CAM-Kok ~~, both of which exhibit large~~

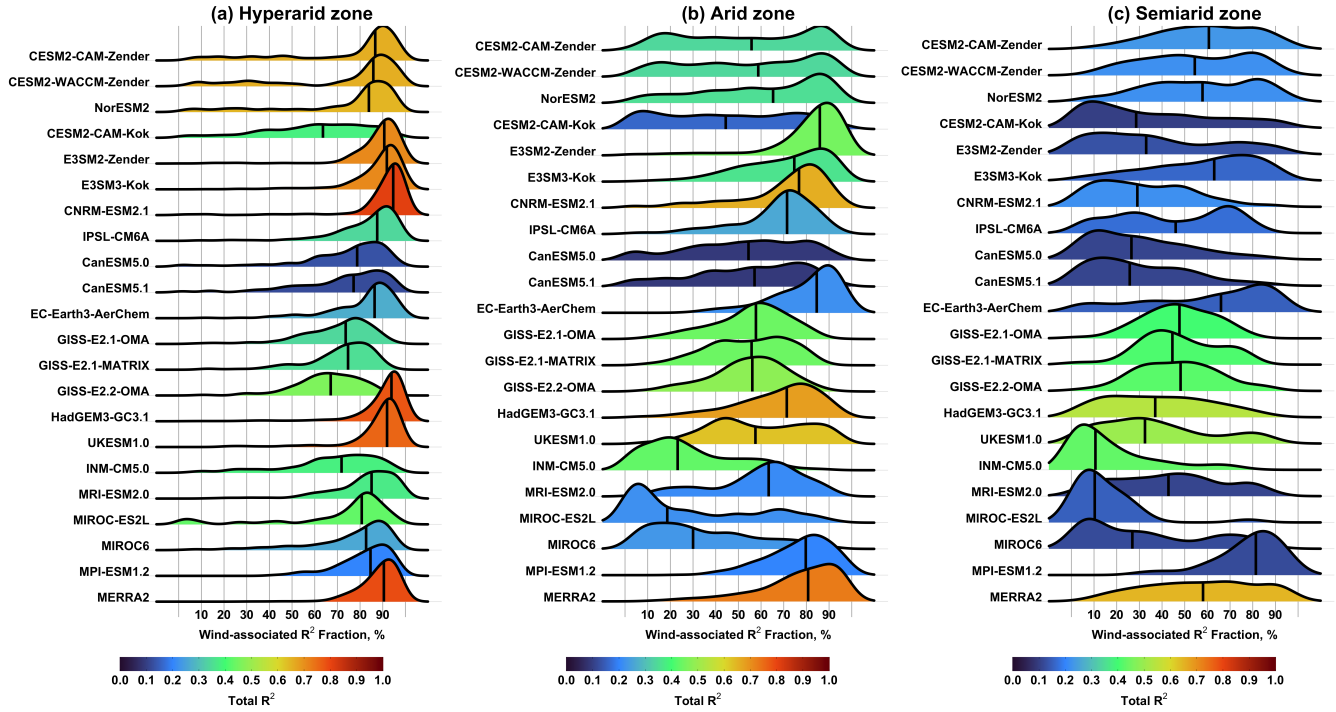

Figure 10. Ridgeline plots ~~of~~ for the fractional contributions of wind speed to the total R^2 over (a) hyperarid, (b) arid, and (c) semiarid climate zones. ~~The median and mean values are denoted by red and blue~~ Black vertical lines ~~, respectively~~indicate median values. Color shading ~~represent the~~ represents mean total R^2 values.

~~variability and low median values. In particular, GFDL-ESM4 yields a median wind R^2 fraction of 42%, indicating an overestimated sensitivity to hydroclimate drivers in the hyperarid zone, particularly over North Africa, Arabian Peninsula and Iranian Plateau (Fig. 8i). Similarly, CESM2-CAM-Kok~~ exhibits ~~large spatial variability~~ greater spatial variability and lower wind influence with a median ~~wind~~ wind-associated R^2 fraction of ~~64%, driven by dominant~~ 63%, consistent with the model's elevated hydroclimate influence over West Africa and the Tarim Basin ~~(~~as shown in Fig. 8b~~). In comparison~~. Compared to CESM2-CAM-Kok, CESM2-CAM-Zender captures the ~~dominant wind influence~~ expected wind dominance with a median ~~value of 86~~of 87%. The ~~suboptimal performance of~~ enhanced hydroclimate influence in CESM2-CAM-Kok relative to CESM2-CAM-Zender persists even when comparing common ~~dust-producing areas in the~~ dust-emitting areas in these two models.

In the arid zone (Fig. 10b), ~~the~~ total R^2 ~~is generally smaller due to~~ values are generally lower, again reflecting reduced explanatory power of the selected predictors. The ESMs ~~also show larger disagreement~~ exhibit greater discrepancies in the relative importance of wind ~~and hydroclimate drivers . The influence of wind speed is reduced and more variable, but still remains dominant~~ speed versus hydroclimate drivers in the arid zone. Specifically, wind speed remains the dominant driver of dust variability in most ESMs~~and MERRA2. The~~ , despite increased spatial variability. The three GISS-E2 models ~~produce relatively equal importance of~~ simulate nearly equal wind and hydroclimate ~~drivers. In contrast, four models—GFDL-ESM4,~~

influences. INM-CM5.0, MIROC-ES2L and ~~MIROC6—yield dominant hydroclimate influence with the median wind~~ MIROC6 produce median wind-associated R^2 ~~fraction falling~~ fractions well below 50%, ~~indicating~~ signifying a transition from wind- to hydroclimate-dominated regimes. CESM2-CAM-Kok also ~~reflects~~ displays this transition, although to a smaller extent with a median ~~value of 46%~~ of 44% and large spatial variability. In both CESM and E3SM, ~~switching from the Zender to Kok scheme results in weaker wind and stronger hydroclimate influences, likely due to the physically based soil erodibility treatment~~ replacing the Zender with Kok dust scheme weakens the wind influence and strengthens the hydroclimate influence, with the median wind-associated R^2 fraction declining from 56% to 44% in CESM and from 86% to 74% in E3SM. This is somewhat consistent with previous findings that the more physically based sediment erodibility formulations in the Kok scheme ~~which enhances~~ enhance the dust sensitivity to ~~hydroclimate variability , as previously suggested in ?~~climate variability relative to the Zender scheme (Kok et al., 2014a).

Results for the semiarid zone (Fig. 10c) are considered less robust due to significantly smaller dust-emitting areas ~~or model grid cells (~~(see Fig. 1). ~~In general, the wind influence further declines~~Overall, the contribution of wind speed further weakens, while hydroclimate ~~divers~~ drivers become more important. The ~~magnitude of this shift~~resulting change of predictor relative importance, however, varies ~~widely, leading to larger discrepancies~~considerably. Specifically, ~~hydroclimate drivers continue to dominate~~ four models (CESM2-CAM-Zender, E3SM3-Kok, EC-Earth3-AerChem and MPI-ESM1.2) retain the wind dominance, albeit with increased spatial variability. Hydroclimate dominance persists and strengthens in CESM2-CAM-Kok, ~~GFDL-ESM4,~~ INM-CM5.0, MIROC-ES2L and MIROC6, ~~same as~~ consistent with their behaviors in the arid zone. ~~The following ESMs display a clear transition~~ In contrast, the following models transition from wind- to hydroclimate-dominated regimes: E3SM2-Zender, CNRM-ESM2.1, CanESM5.0, CanESM5.1, HadGEM3-GC3.1, ~~and~~ UKESM1.0 and MRI-ESM2.0. ~~IPSL-CM6A and~~ GISS-E2 models ~~also show increased~~ and IPSL-CM6A exhibit moderate increases of hydroclimate influence, ~~though to a lesser extent. The remaining ESMs and MERRA2 continue to display dominance of wind speed, albeit with increased spatial variability~~resulting in roughly equal importance of wind and hydroclimate drivers. Compared to the ESMs, MERRA-2 generally produces dominant wind influence across all three climate zones.

~~The above analysis indicates that GFDL-ESM4 and CESM2-CAM-Kok simulate anomalously strong hydroclimate influence in the hyperarid zone.~~ To identify the ~~specific drivers of these anomalies~~sources of hydroclimate influence in the ESMs, Fig. 11 presents the median fractional contributions of five hydroclimate variables to the total R^2 in each model. The contribution attributed to specific humidity can largely be interpreted as a soil moisture effect, given the strong coupling between near-surface humidity and surface soil water content through evapotranspiration. In hyperarid regions, dust variability is expected to be dominated by wind speed, with minimal hydroclimate influence. ~~In the hyperarid zone, most ESMs capture the negligible sensitivity of dust emission to hydroclimate variables. Several exceptions exist, however. CESM2-CAM-Kok shows unusually strong influence from precipitation and specific humidity , while GFDL-ESM4 exhibits anomalously strong sensitivity to soil moisture. The GISS-E2 models display moderately elevated sensitivity to soil moisture and specific humidity, which explains their moderate wind influence in the hyperarid zone (Fig. 10a).~~

~~The overestimation of hydroclimate influence in the hyperarid zone~~ Thus, anomalously large hydroclimate contributions in some ESMs may be explained by ~~a combination of two~~ two possible mechanisms: (1) the ~~hydroclimate variability is~~

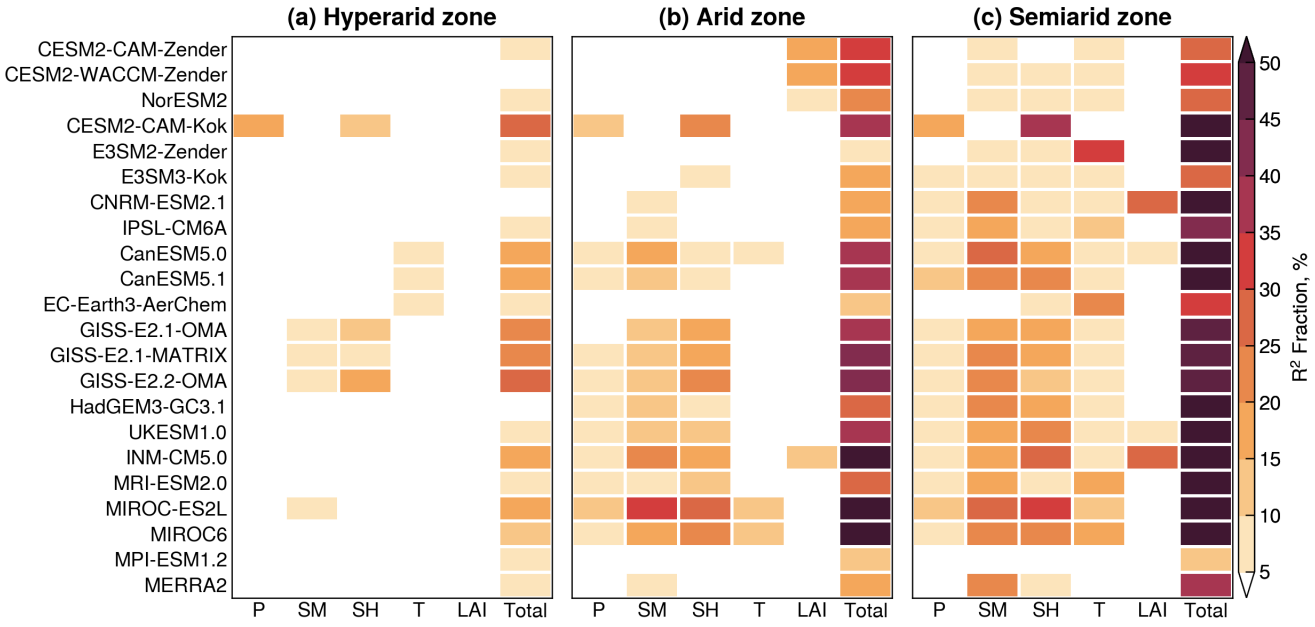

Figure 11. Median factional contributions of hydroclimate ~~variables~~ drivers to the total explained variance (R^2) in Earth system models and ~~MERRA-2~~ MERRA-2 over (a) hyperarid, (b) arid, and (c) semiarid climate zones. Hydroclimate variables are precipitation (P), soil moisture (SM), specific humidity (SH), air temperature (T), and leaf area index (LAI).

~~overestimated in the model, which induces spurious effects on dust emissions ; or~~ model overestimates hydroclimate variability, thereby producing spurious correlations with dust emissions regardless of whether the hydroclimate variable is explicitly used in the dust parameterizations; and (2) the ~~hydroclimate variability is reasonably captured, but the dust scheme incorporates overly strong sensitivity to hydroclimate drivers. ? reported that the GFDL-ESM4 land model significantly overestimates soil moisture over dryland regions, with values more than double those from satellite observations in dust source regions like the central Sahara and Tarim Basin. This bias likely explains the strong apparent sensitivity of dust emission to soil moisture in GFDL-ESM4 (Fig. 11a).~~ model reasonably represents hydroclimate variability but overestimates dust sensitivity to the hydroclimate variable, indicating a potential bias in the parameterization itself. Understanding the causes for the statistically inferred predictor influences would require detailed knowledge of the physical parameterizations and model configurations specific to each ESM.

~~The abnormal~~ In the hyperarid zone, the hydroclimate influence in CESM2-CAM-Kok ~~may be partly explained by dust emission parameterizations~~ is associated with precipitation and specific humidity, which may partly reflect the increased dust sensitivity to soil moisture in the Kok scheme ~~, which introduces enhanced sensitivity to the threshold wind velocity compared to the Zender scheme (?). Because of this heightened dependence on land surface conditions, the Kok scheme does not require predefined dust source functions and is considered more physically realistic for projecting dust responses to future climate and land-use changes.~~ relative to the Zender scheme (Kok et al., 2014a). Another possible reason is the ~~relatively~~ short simulation

period ~~in~~ for CESM2-CAM-Kok (2004–2013), which may not ~~fully capture the long-term~~ adequately capture the full range of dust variability and predictor ~~influence~~ relationships as in CESM2-CAM-Zender (1980–2014). In this regard, the E3SM experiments provide a more robust comparison between the ~~Zender and Kok~~ two dust schemes. As shown in Fig. 11a, ~~the E3SM models exhibit~~ both E3SM2-Zender and E3SM3-Kok produce the expected negligible hydroclimate influence in the hyperarid zone~~, regardless of the dust scheme used~~. In the arid zone, however, E3SM3-Kok ~~shows higher~~ exhibits stronger hydroclimate influence than E3SM2-Zender~~due to increased sensitivity to specific humidity (Fig. 11b). This comparison provides additional evidence~~ , consistent with previous findings that the Kok scheme amplifies the dust ~~emission~~ sensitivity to hydroclimate conditions ~~.~~ compared to the Zender scheme (Kok et al., 2014a). GISS models exhibit elevated influences from specific humidity and soil moisture, which explains their moderate wind contributions as shown in Fig. 10a.

In the arid zone (Fig. 11b), ~~most ESMs show enhanced influence from~~ the enhanced hydroclimate influence is primarily associated with soil moisture and specific humidity in most ESMs, consistent with ~~empirical evidence that both variables strongly affect the soil erodibility and wind erosion risk (e.g., **???**). Interpreting the LAI influence, however, is more complex due to several factors. First, unlike~~ their well-established roles in modulating sediment erodibility (e.g., Csavina et al., 2014; Ravi et al., 200 . Several models—including CESM and INM-CM5.0—attribute strong influences to LAI. Unlike other hydroclimate variables, LAI ~~can be either~~ may be prescribed from climatology or ~~simulated by the model's dynamic vegetation component~~ interactively simulated by dynamic vegetation model components (Table 1). Models using prescribed LAI ~~are expected to show minimal interannual variability and hence limited~~ typically exhibit limited interannual variability in vegetation cover and therefore weak influence on dust emissions. ~~Second, the LAI effect on dust emission is treated differently. For example, CESM assumes a linear relationship between bare soil fraction and LAI when LAI is below 0.3, while GFDL-ESM4 assumes an exponential decrease in bare soil fraction as a function of LAI. Because LAI is often used to derive bare soil fraction in vertical dust flux calculations, these differences can alter the modeled dust sensitivity to vegetation cover. Most ESMs in Fig. 11b exhibit weak to negligible LAI influence , likely reflecting either prescribed LAI or the normalization of dust fluxes prior to dominance analysis (see Section 2). One outlier is GFDL-ESM4 which exhibits the strongest sensitivity to LAI, even well above the sensitivity to soil moisture. This~~ For CESM and INM-CM5.0, the elevated LAI influence can be explained by ~~the strong coupled between LAI and dust emission in the model, and the fact that no normalization was applied to GFDL-ESM4 due to missing~~ their parameterizations of the bare soil fraction ~~output from the CMIP6 archive~~as a function of LAI.

4 Conclusions

This study ~~evaluates discrepancies and biases~~ examines discrepancies among 21 ESMs in representing the interannual variability of windblown dust emissions and the relative importance of near-surface wind speed ~~and~~ versus five hydroclimate drivers (precipitation, soil moisture, specific humidity, air temperature, and LAI) ~~. We treat dust emission flux as an unobservable, model-specific quantity and use dominance analysis to quantify the variance explained in dust emission fluxes by wind and hydroclimate drivers within each model. The analysis is conducted over three climatologically defined climate~~ across different climate aridity zones (hyperarid, arid, and semiarid)~~, and further examines the effect~~ . Recognizing the unconstrained,

model-specific nature of dust emission ~~parameterizations through paired CESM and E3SM experiments with the ? and ? schemes~~fluxes, we use the dominance analysis technique to quantify the relative influence of a common set of six physical drivers within each model.

The ~~hyperarid zone contributes more than half of global dust emissions in all models except CanESM5.1 and INM-CM5.0, which simulate relatively spatially even emission patterns with less than 50% from the hyperarid zone, likely due to known deficiencies and over-simplifications in dust emission representations~~extent of inter-model agreement in dust variability varies strongly with climate aridity. In the hyperarid zone, the ESMs exhibit poor agreement~~with each other and with MERRA2 in simulating the dust variability~~, with only ~~10% of pairwise model comparisons yielding statistically significant , positive correlations~~9% out of 210 pairwise comparisons showing statistically significant positive correlations, reflecting large inconsistencies in model-simulated near-surface wind speeds. In arid and semiarid zones, the ESMs exhibit a ~~dipole pattern with both improved agreement and increased disagreement. This behavior can be explained~~ dual pattern driven by a "double-edged sword" effect of land surface memory: models with coherent representations of hydroclimate variability tend to converge in their simulated dust variability, ~~while~~ whereas those with divergent hydroclimate representations diverge in dust emission responses.

The relative ~~influence of wind and~~ importance of wind speed versus hydroclimate drivers also varies with climate ~~regimes. Most~~ aridity. In hyperarid areas, most ESMs capture the ~~dominant control~~ expected dominance of wind speed and ~~weak sensitivity to hydroclimate conditions in the hyperarid zone, except~~ minimal hydroclimate influence. CESM2-CAM-Kok exhibits elevated influences from precipitation and ~~GFDL-ESM4, both of which show great spatial variability and abnormally strong influencefrom precipitation,~~ specific humidity, ~~and soil moisture. The overestimated hydroclimate influence in GFDL-ESM4 can be explained by the model's overestimation of soil moisture and consequent spurious effects on dust emissions. The enhanced hydroclimate influence in CESM2-CAM-Kok (relative to CESM2-CAM-Zender) may be explained, at least partly , by the physically based soil~~ which may partly result from the more physically based sediment erodibility formulations in the ~~? scheme , which replaces the use of predefined dust source functions~~Kok et al. (2014b) scheme relative to the Zender et al. (2003) scheme. A similar ~~pattern~~ behavior is found in E3SM, where ~~switching from the ? to the ? scheme strengthens the hydroclimate influence in the arid zone. However, due to concurrent updates in model physics (e.g., dust mineralogy, radiative feedbacks, and meteorology), further experiments are~~ replacing the Zender et al. (2003) scheme with the Kok et al. (2014b) scheme reduces the wind dominance and enhances the hydroclimate influence on dust emission. Due to confounding model changes in the CESM and E3SM experiments, however, targeted experiments will be needed to isolate the ~~effects of dust emission parameterizations on dust–climate sensitivities.~~

effect of dust parameterization choice on the dust sensitivity. In arid and semiarid ~~zones, the influence of wind speed~~ areas, wind influence generally weakens while ~~the~~ hydroclimate influence strengthens in all ESMs. However, the relative importance ~~of wind and hydroclimate drivers becomes increasingly inconsistent between the models, with an increasing number of ESMs shifting toward comparable or dominant-dominated regimes. In general, MERRA2 produces~~ between the two becomes less consistent, with contrasting model behaviors in retaining wind dominance or shifting toward hydroclimate dominance or near-equal importance. Compared to the ESMs, the MERRA-2 aerosol reanalysis generally produce stronger wind influence and weaker hydroclimate influence ~~than the ESMs.~~ across all climate regimes.

~~In summary, this study provides new~~ Note that the physical drivers considered in this study may not fully represent all the dust emission driving factors for specific emission schemes; instead, we focus on a common set of drivers for all models to provide a fair comparison across the ESMs. Therefore, the inferred relative importance from this analysis is limited to those common drivers considered and their influences on dust emissions in different models. Also, because of the statistical nature of dominance analysis, the predictor importance results shall be interpreted with caution when linking to model parameterizations. Despite these limitations, this study introduces a new framework for model intercomparison and yields new insights into how current ESMs represent the ~~temporal~~ variability and physical ~~drivers of windblown dust emissions . Most ESMs capture the dominant wind control over permanently dry, barren surfaces, their poor agreement in dust variability highlights large inconsistencies in the simulated~~ controls of dust emissions across different climate aridity regimes. Overall, our findings highlight two promising directions for reducing model uncertainties in dust emission simulations: (1) improving the representation of near-surface ~~winds. The dipole model behavior in arid and semiarid zones underscores the important role of hydroclimate variability~~ wind speeds and gustiness in hyperarid regions, and (2) enhancing the representation of hydroclimate and land surface processes ~~. Improving model representations of soil and vegetation dynamics and dust-climate interactions in these regions is essential for reducing uncertainties in future projections of dust emissions under changing climate and land-use conditions~~that modulate sediment erodibility in arid and semiarid areas.

Data availability. Model comparison and dominance analysis results are available at https://doi.org/10.5281/zenodo.17666380.

Author contributions. Conceptualization and methodology - Xin Xi; Data curation and analysis - Xinzhu Li, Xin Xi, Longlei Li, Yan Feng; Writing of original draft - Xinzhu Li, Xin Xi. Review and editing of draft - Xinzhu Li, Xin Xi, Longlei Li, Yan Feng.

Competing interests. The authors declare no competing interests.

Acknowledgements. X.L. and X.X. are partially supported by ~~the~~ NASA Land-Cover and Land-Use Change Program (grant 80NSSC20K1480). Y.F. acknowledges the support of the Energy Exascale Earth System Model (E3SM) project, funded by the U.S. Department of Energy (DOE), Office of Science, Office of Biological and Environmental Research~~. The work at Argonne National Laboratory was supported by the U.S. DOE Office of Science~~ , under contract DE-AC02-06CH11357. All authors thank the E3SM project team for their efforts in developing and supporting the E3SM. L.L. acknowledges support from ~~the U.S. Department of Energy (DOE)~~ DOE under award DE-SC0021302, and from the Earth Surface Mineral Dust Source Investigation (EMIT), a ~~National Aeronautics and Space Administration (NASA)~~ NASA Earth Ventures-Instrument (EVI-4) mission. He also acknowledges the high-performance computing resources provided by Derecho at the National Center for Atmospheric Research (NCAR), through NCAR's Computational and Information Systems Laboratory (CISL), which is sponsored by the National Science Foundation (NSF). ~~The~~ All authors acknowledge the World Climate Research Programme for coordinat-

ing and promoting CMIP6, and thank the climate modeling groups for producing and making available their model output, the Earth System Grid Federation (ESGF) for archiving the data and providing access, and the multiple funding agencies who support CMIP6 and ESGF.

References

Albani, S., Mahowald, N. M., Perry, A. T., Scanza, R. A., Zender, C. S., Heavens, N. G., Maggi, V., Kok, J. F., and Otto-Bliesner, B. L.: Improved dust representation in the Community Atmosphere Model, Journal of Advances in Modeling Earth Systems, 6, 541–570, https://doi.org/10.1002/2013MS000279, 2015.

Aryal, Y. N. and Evans, S.: Global Dust Variability Explained by Drought Sensitivity in CMIP6 Models, Journal of Geophysical Research: Earth Surface, 126, https://doi.org/10.1029/2021JF006073, 2021.

Azen, R. and Budescu, D. V.: The Dominance Analysis Approach for Comparing Predictors in Multiple Regression, Psychological Methods, 8, 129–148, https://doi.org/10.1037/1082-989X.8.2.129, 2003.

Bagnold, R. A.: The Physics of Blown Sand and Desert Dunes, Springer Dordrecht, 1 edn., ISBN 978-94-009-5684-1, https://doi.org/10.1007/978-94-009-5682-7, 1974.

Balkanski, Y., Schulz, M., Claquin, T., Moulin, C., and Ginoux, P.: Global Emissions of Mineral Aerosol: Formulation and Validation using Satellite Imagery, in: Emissions of Atmospheric Trace Compounds, edited by Granier, C., Artaxo, P., and Reeves, C. E., pp. 239–267, Springer, https://doi.org/10.1007/978-1-4020-2167-1_6, 2004.

Bauer, S. E., Tsigaridis, K., Faluvegi, G., Nazarenko, L., Miller, R. L., Kelley, M., and Schmidt, G.: The Turning Point of the Aerosol Era, Journal of Advances in Modeling Earth Systems, 14, https://doi.org/10.1029/2022MS003070, 2022.

Budescu, D. V.: Dominance analysis: A new approach to the problem of relative importance of predictors in multiple regression, Psychological Bulletin, 114, 542–551, https://doi.org/10.1037/0033-2909.114.3.542, 1993.

Bullard, J. E. and Livingstone, I.: Interactions between aeolian and fluvial systems in dryland environments, Area, 34, 8–16, https://doi.org/10.1111/1475-4762.00052, 2002.

Bullard, J. E., Harrison, S. P., Baddock, M. C., Drake, N., Gill, T. E., McTainsh, G., and Sun, Y.: Preferential dust sources: A geomorphological classification designed for use in global dust-cycle models, Journal of Geophysical Research: Earth Surface, 116, https://doi.org/10.1029/2011JF002061, 2011.

Cowie, S. M., Marsham, J. H., and Knippertz, P.: The importance of rare, high-wind events for dust uplift in northern Africa, Geophysical Research Letters, 42, 8208–8215, https://doi.org/10.1002/2015GL065819, 2015.

Csavina, J., Field, J., Félix, O., Corral-Avitia, A. Y., Sáez, A. E., and Betterton, E. A.: Effect of wind speed and relative humidity on atmospheric dust concentrations in semi-arid climates, Science of the Total Environment, 487, 82–90, https://doi.org/10.1016/j.scitotenv.2014.03.138, 2014.

Engelstaedter, S., Kohfeld, K. E., Tegen, I., and Harrison, S. P.: Controls of dust emissions by vegetation and topographic depressions: An evaluation using dust storm frequency data, Geophysical Research Letters, 30, https://doi.org/10.1029/2002GL016471, iSBN: 0094-8276, 2003.

Evan, A. T.: Surface Winds and Dust Biases in Climate Models, Geophysical Research Letters, 45, 1079–1085, https://doi.org/10.1002/2017GL076353, 2018.

Evan, A. T., Flamant, C., Fiedler, S., and Doherty, O.: An analysis of aeolian dust in climate models, Geophysical Research Letters, 41, 5996–6001, https://doi.org/10.1002/2014GL060545, 2014.

Evans, S., Ginoux, P., Malyshev, S., and Shevliakova, E.: Climate-vegetation interaction and amplification of Australian dust variability, Geophysical Research Letters, 43, 11,823–11,830, https://doi.org/10.1002/2016GL071016, publisher: John Wiley & Sons, Ltd, 2016.

Feng, Y., Wang, H., Rasch, P. J., Zhang, K., Lin, W., Tang, Q., Xie, S., Hamilton, D. S., Mahowald, N., and Yu, H.: Global Dust Cycle and Direct Radiative Effect in E3SM Version 1: Impact of Increasing Model Resolution, Journal of Advances in Modeling Earth Systems, https://doi.org/10.1029/2021MS002909, 2022.

Fécan, F., Marticorena, B., and Bergametti, G.: Parametrization of the increase of the aeolian erosion threshold wind friction velocity due to soil moisture for arid and semi-arid areas, Annales Geophysicae, 17, 149, https://doi.org/10.1007/s005850050744, 1999.

Gelaro, R., McCarty, W., Suárez, M. J., Todling, R., Molod, A., Takacs, L., Randles, C. A., Darmenov, A., Bosilovich, M. G., Reichle, R., Wargan, K., Coy, L., Cullather, R., Draper, C., Akella, S., Buchard, V., Conaty, A., Silva, A. M. d., Gu, W., Kim, G. K., Koster, R., Lucchesi, R., Merkova, D., Nielsen, J. E., Partyka, G., Pawson, S., Putman, W., Rienecker, M., Schubert, S. D., Sienkiewicz, M., and Zhao, B.: The modern-era retrospective analysis for research and applications, version 2 (MERRA-2), Journal of Climate, 30, 5419–5454, https://doi.org/10.1175/JCLI-D-16-0758.1, 2017.

Gettelman, A., Mills, M. J., Kinnison, D. E., Garcia, R. R., Smith, A. K., Marsh, D. R., Tilmes, S., Vitt, F., Bardeen, C. G., McInerny, J., Liu, H. L., Solomon, S. C., Polvani, L. M., Emmons, L. K., Lamarque, J. F., Richter, J. H., Glanville, A. S., Bacmeister, J. T., Phillips, A. S., Neale, R. B., Simpson, I. R., DuVivier, A. K., Hodzic, A., and Randel, W. J.: The Whole Atmosphere Community Climate Model Version 6 (WACCM6), Journal of Geophysical Research: Atmospheres, 124, 12 380–12 403, https://doi.org/10.1029/2019JD030943, publisher: Blackwell Publishing Ltd, 2019.

Ginoux, P., Chin, M., Tegen, I., Prospero, J. M., Holben, B., Dubovik, O., and Lin, S. J.: Sources and distributions of dust aerosols simulated with the GOCART model, Journal of Geophysical Research Atmospheres, 106, 20 255–20 273, https://doi.org/10.1029/2000JD000053, 2001.

Gliß, J., Mortier, A., Schulz, M., Andrews, E., Balkanski, Y., Bauer, S. E., Benedictow, A. M. K., Bian, H., Checa-Garcia, R., Chin, M., Ginoux, P., Griesfeller, J. J., Heckel, A., Kipling, Z., Kirkeväg, A., Kokkola, H., Laj, P., Sager, P. L., Lund, M. T., Myhre, C. L., Matsui, H., Myhre, G., Neubauer, D., Noije, T. V., North, P., Olivié, D. J. L., Rémy, S., Sogacheva, L., Takemura, T., Tsigaridis, K., and Tsyro, S. G.: AeroCom phase III multi-model evaluation of the aerosol life cycle and optical properties using ground- And space-based remote sensing as well as surface in situ observations, Atmospheric Chemistry and Physics, 21, 87–128, https://doi.org/10.5194/acp-21-87-2021, 2021.

Hajima, T., Watanabe, M., Yamamoto, A., Tatebe, H., Noguchi, M. A., Abe, M., Ohgaito, R., Ito, A., Yamazaki, D., Okajima, H., Ito, A., Takata, K., Ogochi, K., Watanabe, S., and Kawamiya, M.: Development of the MIROC-ES2L Earth system model and the evaluation of biogeochemical processes and feedbacks, Geoscientific Model Development, 13, 2197–2244, https://doi.org/10.5194/gmd-13-2197-2020, 2020.

Huneeus, N., Schulz, M., Balkanski, Y., Griesfeller, J., Prospero, J., Kinne, S., Bauer, S., Boucher, O., Chin, M., Dentener, F., Diehl, T., Easter, R., Fillmore, D., Ghan, S., Ginoux, P., Grini, A., Horowitz, L., Koch, D., Krol, M. C., Landing, W., Liu, X., Mahowald, N., Miller, R., Morcrette, J. J., Myhre, G., Penner, J., Perlwitz, J., Stier, P., Takemura, T., and Zender, C. S.: Global dust model intercomparison in AeroCom phase i, Atmospheric Chemistry and Physics, 11, 7781–7816, https://doi.org/10.5194/acp-11-7781-2011, iSBN: 1680-7324 Publisher: Copernicus Publications, 2011.

Kim, D., Chin, M., Yu, H., Diehl, T., Tan, Q., Kahn, R. A., Tsigaridis, K., Bauer, S. E., Takemura, T., Pozzoli, L., Bellouin, N., Schulz, M., Peyridieu, S., Chédin, A., and Koffi, B.: Sources, sinks, and transatlantic transport of North African dust aerosol: A multimodel analysis and comparison with remote sensing data, Journal of Geophysical Research, 119, 6259–6277, https://doi.org/10.1002/2013JD021099, 2014.

Kim, D., Chin, M., Schuster, G., Yu, H., Takemura, T., Tuccella, P., Ginoux, P., Liu, X., Shi, Y., Matsui, H., Tsigaridis, K., Bauer, S. E., Kok, J. F., and Schulz, M.: Where Dust Comes From: Global Assessment of Dust Source Attributions With AeroCom Models, Journal of Geophysical Research: Atmospheres, 129, e2024JD041 377, https://doi.org/https://doi.org/10.1029/2024JD041377, publisher: John Wiley & Sons, Ltd, 2024.

Kim, H. and Choi, M.: Impact of soil moisture on dust outbreaks in East Asia: Using satellite and assimilation data, Geophysical Research Letters, 42, 2789–2796, https://doi.org/https://doi.org/10.1002/2015GL063325, publisher: John Wiley & Sons, Ltd, 2015.

Knippertz, P. and Todd, M. C.: Mineral dust aerosols over the Sahara: Meteorological controls on emission and transport and implications for modeling, Reviews of Geophysics, 50, https://doi.org/10.1029/2011RG000362, 2012.

Kok, J. F., Parteli, E. J. R., Michaels, T. I., and Karam, D. B.: The physics of wind-blown sand and dust, Reports on Progress in Physics, 75, https://doi.org/10.1088/0034-4885/75/10/106901, 2012.

Kok, J. F., Albani, S., Mahowald, N. M., and Ward, D. S.: An improved dust emission model - Part 2: Evaluation in the Community Earth System Model, with implications for the use of dust source functions, Atmospheric Chemistry and Physics, 14, 13 043–13 061, https://doi.org/10.5194/acp-14-13043-2014, 2014a.

Kok, J. F., Mahowald, N. M., Fratini, G., Gillies, J. A., Ishizuka, M., Leys, J. F., Mikami, M., Park, M. S., Park, S. U., Pelt, R. S. V., and Zobeck, T. M.: An improved dust emission model - Part 1: Model description and comparison against measurements, Atmospheric Chemistry and Physics, 14, 13 023–13 041, https://doi.org/10.5194/acp-14-13023-2014, 2014b.

Kok, J. F., Storelvmo, T., Karydis, V. A., Adebiyi, A. A., Mahowald, N. M., Evan, A. T., He, C., and Leung, D. M.: Mineral dust aerosol impacts on global climate and climate change, Nature Reviews Earth and Environment, 4, 71–86, https://doi.org/10.1038/s43017-022-00379-5, 2023.

Koster, R. D., Guo, Z., Yang, R., Dirmeyer, P. A., Mitchell, K., and Puma, M. J.: On the nature of soil moisture in land surface models, Journal of Climate, 22, 4322–4335, https://doi.org/10.1175/2009JCLI2832.1, 2009.

Leung, D. M., Kok, J. F., Li, L., Okin, G. S., Prigent, C., Klose, M., García-Pando, C. P., Menut, L., Mahowald, N. M., Lawrence, D. M., and Chamecki, M.: A new process-based and scale-aware desert dust emission scheme for global climate models - Part I: Description and evaluation against inverse modeling emissions, Atmospheric Chemistry and Physics, 23, 6487–6523, https://doi.org/10.5194/acp-23-6487-2023, 2023.

Li, L., Mahowald, N. M., Kok, J. F., Liu, X., Wu, M., Leung, D. M., Hamilton, D. S., Emmons, L. K., Huang, Y., Sexton, N., Meng, J., and Wan, J.: Importance of different parameterization changes for the updated dust cycle modeling in the Community Atmosphere Model (version 6.1), Geoscientific Model Development, 15, 8181–8219, https://doi.org/10.5194/gmd-15-8181-2022, 2022.

Li, L., Mahowald, N. M., Ageitos, M. G., Obiso, V., Miller, R. L., García-Pando, C. P., Biagio, C. D., Formenti, P., Brodrick, P. G., Clark, R. N., Green, R. O., Kokaly, R., Swayze, G., and Thompson, D. R.: Improved constraints on hematite refractive index for estimating climatic effects of dust aerosols, Communications Earth & Environment, 5, 295, https://doi.org/10.1038/s43247-024-01441-4, 2024.

Lurton, T., Balkanski, Y., Bastrikov, V., Bekki, S., Bopp, L., Braconnot, P., Brockmann, P., Cadule, P., Contoux, C., Cozic, A., Cugnet, D., Dufresne, J.-L., Éthé, C., Foujols, M.-A., Ghattas, J., Hauglustaine, D., Hu, R.-M., Kageyama, M., Khodri, M., Lebas, N., Levavasseur, G., Marchand, M., Ottlé, C., Peylin, P., Sima, A., Szopa, S., Thiéblemont, R., Vuichard, N., and Boucher, O.: Implementation of the CMIP6 Forcing Data in the IPSL-CM6A-LR Model, Journal of Advances in Modeling Earth Systems, 12, e2019MS001 940, https://doi.org/https://doi.org/10.1029/2019MS001940, publisher: John Wiley & Sons, Ltd, 2020.

Marticorena, B. and Bergametti, G.: Modeling the atmospheric dust cycle: 1. Design of a soil-derived dust emission scheme, Journal of Geophysical Research, 100, https://doi.org/10.1029/95jd00690, 1995.

Mauritsen, T., Bader, J., Becker, T., Behrens, J., Bittner, M., Brokopf, R., Brovkin, V., Claussen, M., Crueger, T., Esch, M., Fast, I., Fiedler, S., Fläschner, D., Gayler, V., Giorgetta, M., Goll, D. S., Haak, H., Hagemann, S., Hedemann, C., Hohenegger, C., Ilyina, T., Jahns, T., Jimenéz-de-la Cuesta, D., Jungclaus, J., Kleinen, T., Kloster, S., Kracher, D., Kinne, S., Kleberg, D., Lasslop, G., Kornblueh, L., Marotzke, J., Matei, D., Meraner, K., Mikolajewicz, U., Modali, K., Möbis, B., Müller, W. A., Nabel, J. E. M. S., Nam, C. C. W., Notz, D., Nyawira, S.-S., Paulsen, H., Peters, K., Pincus, R., Pohlmann, H., Pongratz, J., Popp, M., Raddatz, T. J., Rast, S., Redler, R., Reick, C. H., Rohrschneider, T., Schemann, V., Schmidt, H., Schnur, R., Schulzweida, U., Six, K. D., Stein, L., Stemmler, I., Stevens, B., Storch, J.-S. v., Tian, F., Voigt, A., Vrese, P., Wieners, K.-H., Wilkenskjeld, S., Winkler, A., and Roeckner, E.: Developments in the MPI-M Earth System Model version 1.2 (MPI-ESM1.2) and Its Response to Increasing CO2, Journal of Advances in Modeling Earth Systems, 11, 998–1038, https://doi.org/https://doi.org/10.1029/2018MS001400, publisher: John Wiley & Sons, Ltd, 2019.

Miller, R. L., Cakmur, R. V., Perlwitz, J., Geogdzhayev, I. V., Ginoux, P., Koch, D., Kohfeld, K. E., Prigent, C., Ruedy, R., Schmidt, G. A., and Tegen, I.: Mineral dust aerosols in the NASA Goddard Institute for Space Sciences ModelE atmospheric general circulation model, Journal of Geophysical Research Atmospheres, 111, https://doi.org/10.1029/2005JD005796, 2006.

Miller, R. L., Schmidt, G. A., Nazarenko, L. S., Bauer, S. E., Kelley, M., Ruedy, R., Russell, G. L., Ackerman, A. S., Aleinov, I., Bauer, M., Bleck, R., Canuto, V., Cesana, G., Cheng, Y., Clune, T. L., Cook, B. I., Cruz, C. A., Genio, A. D. D., Elsaesser, G. S., Faluvegi, G., Kiang, N. Y., Kim, D., Lacis, A. A., Leboissetier, A., LeGrande, A. N., Lo, K. K., Marshall, J., Matthews, E. E., McDermid, S., Mezuman, K., Murray, L. T., Oinas, V., Orbe, C., García-Pando, C. P., Perlwitz, J. P., Puma, M. J., Rind, D., Romanou, A., Shindell, D. T., Sun, S., Tausnev, N., Tsigaridis, K., Tselioudis, G., Weng, E., Wu, J., and Yao, M. S.: CMIP6 Historical Simulations (1850–2014) With GISS-E2.1, Journal of Advances in Modeling Earth Systems, 13, https://doi.org/10.1029/2019MS002034, 2021.

Nandintsetseg, B. and Shinoda, M.: Land surface memory effects on dust emission in a Mongolian temperate grassland, Journal of Geophysical Research: Biogeosciences, 120, 414–427, https://doi.org/10.1002/2014JG002708, 2015.

Noije, T. V., Bergman, T., Sager, P. L., O'Donnell, D., Makkonen, R., Gonçalves-Ageitos, M., Döscher, R., Fladrich, U., Hardenberg, J. V., Keskinen, J. P., Korhonen, H., Laakso, A., Myriokefalitakis, S., Ollinaho, P., Garciá-Pando, C. P., Reerink, T., Schrödner, R., Wyser, K., and Yang, S.: EC-Earth3-AerChem: A global climate model with interactive aerosols and atmospheric chemistry participating in CMIP6, Geoscientific Model Development, 14, 5637–5668, https://doi.org/10.5194/gmd-14-5637-2021, 2021.

Owen, P. R.: Saltation of uniform grains in air, Journal of Fluid Mechanics, 20, 225–242, https://doi.org/10.1017/S0022112064001173, 1964.

Peng, Y., Salzen, K. V., and Li, J.: Simulation of mineral dust aerosol with Piecewise Log-normal Approximation (PLA) in CanAM4-PAM, Atmospheric Chemistry and Physics, 12, 6891–6914, https://doi.org/10.5194/acp-12-6891-2012, 2012.

Prospero, J. M. and Lamb, P. J.: African Droughts and Dust Transport to the Caribbean: Climate Change Implications, Science, 302, 1024–1027, https://doi.org/10.1126/science.1089915, publisher: American Association for the Advancement of Science, 2003.

Prospero, J. M., Ginoux, P., Torres, O., Nicholson, S. E., and Gill, T. E.: Environmental characterization of global sources of atmospheric soil dust identified with the Nimbus 7 Total Ozone Mapping Spectrometer (TOMS) absorbing aerosol product, Reviews of Geophysics, 40, 2–1–2–31, https://doi.org/10.1029/2000RG000095, iSBN: 8755-1209, 2002.

Pu, B. and Ginoux, P.: The impact of the Pacific Decadal Oscillation on springtime dust activity in Syria, Atmospheric Chemistry and Physics, 16, 13 431–13 448, https://doi.org/10.5194/acp-16-13431-2016, 2016.

Pu, B. and Ginoux, P.: How reliable are CMIP5 models in simulating dust optical depth?, Atmospheric Chemistry and Physics, 18, 12 491–12 510, https://doi.org/10.5194/acp-18-12491-2018, 2018.

Randles, C. A., Silva, A. M. d., Buchard, V., Colarco, P. R., Darmenov, A., Govindaraju, R., Smirnov, A., Holben, B., Ferrare, R., Hair, J., Shinozuka, Y., and Flynn, C. J.: The MERRA-2 aerosol reanalysis, 1980 onward. Part I: System description and data assimilation evaluation, Journal of Climate, 30, 6823–6850, https://doi.org/10.1175/JCLI-D-16-0609.1, 2017.

Raupach, M. R., Gillette, D. A., and Leys, J. F.: The effect of roughness elements on wind erosion threshold, Journal of Geophysical Research: Atmospheres, 98, 3023–3029, https://doi.org/10.1029/92JD01922, 1993.

Ravi, S., Zobeck, T. E. D. M., Over, T. M., Okin, G. S., and D'Odorico, P.: On the effect of moisture bonding forces in air-dry soils on threshold friction velocity of wind erosion, Sedimentology, 53, 597–609, https://doi.org/https://doi.org/10.1111/j.1365-3091.2006.00775.x, publisher: John Wiley & Sons, Ltd, 2006.

Rind, D., Orbe, C., Jonas, J., Nazarenko, L., Zhou, T., Kelley, M., Lacis, A., Shindell, D., Faluvegi, G., Romanou, A., Russell, G., Tausnev, N., Bauer, M., and Schmidt, G.: GISS Model E2.2: A Climate Model Optimized for the Middle Atmosphere—Model Structure, Climatology, Variability, and Climate Sensitivity, Journal of Geophysical Research: Atmospheres, 125, https://doi.org/10.1029/2019JD032204, 2020.

Roberts, M. J., Baker, A., Blockley, E. W., Calvert, D., Coward, A., Hewitt, H. T., Jackson, L. C., Kuhlbrodt, T., Mathiot, P., Roberts, C. D., Schiemann, R., Seddon, J., Vannière, B., and Vidale, P. L.: Description of the resolution hierarchy of the global coupled HadGEM3-GC3.1 model as used in CMIP6 HighResMIP experiments, Geosci. Model Dev., 12, 4999–5028, https://doi.org/10.5194/gmd-12-4999-2019, publisher: Copernicus Publications, 2019.

Seland, O., Bentsen, M., Olivié, D., Toniazzo, T., Gjermundsen, A., Graff, L. S., Debernard, J. B., Gupta, A. K., He, Y. C., Kirkeväg, A., Schwinger, J., Tjiputra, J., Aas, K. S., Bethke, I., Fan, Y., Griesfeller, J., Grini, A., Guo, C., Ilicak, M., Karset, I. H. H., Landgren, O., Liakka, J., Moseid, K. O., Nummelin, A., Spensberger, C., Tang, H., Zhang, Z., Heinze, C., Iversen, T., and Schulz, M.: Overview of the Norwegian Earth System Model (NorESM2) and key climate response of CMIP6 DECK, historical, and scenario simulations, Geoscientific Model Development, 13, 6165–6200, https://doi.org/10.5194/gmd-13-6165-2020, 2020.

Shao, Y.: A model for mineral dust emission, Journal of Geophysical Research Atmospheres, 106, 20 239–20 254, https://doi.org/10.1029/2001JD900171, 2001.

Shao, Y., Raupach, M. R., and Leys, J. F.: A model for predicting aeolian sand drift and dust entrainment on scales from paddock to region, Australian Journal of Soil Research, 34, 309–342, https://doi.org/10.1071/SR9960309, 1996.

Shao, Y., Wyrwoll, K. H., Chappell, A., Huang, J., Lin, Z., McTainsh, G. H., Mikami, M., Tanaka, T. Y., Wang, X., and Yoon, S.: Dust cycle: An emerging core theme in Earth system science, Aeolian Research, 2, 181–204, https://doi.org/10.1016/j.aeolia.2011.02.001, 2011.

Shevliakova, E., Malyshev, S., Martinez-Cano, I., Milly, P. C. D., Pacala, S. W., Ginoux, P., Dunne, K. A., Dunne, J. P., Dupuis, C., Findell, K. L., Ghannam, K., Horowitz, L. W., Knutson, T. R., Krasting, J. P., Naik, V., Phillipps, P., Zadeh, N., Yu, Y., Zeng, F., and Zeng, Y.: The Land Component LM4.1 of the GFDL Earth System Model ESM4.1: Model Description and Characteristics of Land Surface Climate and Carbon Cycling in the Historical Simulation, Journal of Advances in Modeling Earth Systems, 16, e2023MS003 922, https://doi.org/https://doi.org/10.1029/2023MS003922, publisher: John Wiley & Sons, Ltd, 2024.

Shinoda, M. and Nandintsetseg, B.: Soil moisture and vegetation memories in a cold, arid climate, Global and Planetary Change, 79, 110–117, https://doi.org/10.1016/j.gloplacha.2011.08.005, 2011.

Sigmond, M., Anstey, J., Arora, V., Digby, R., Gillett, N., Kharin, V., Merryfield, W., Reader, C., Scinocca, J., Swart, N., Virgin, J., Abraham, C., Cole, J., Lambert, N., Lee, W. S., Liang, Y., Malinina, E., Rieger, L., Salzen, K. V., Seiler, C., Seinen, C., Shao, A., Sospedra-Alfonso, R., Wang, L., and Yang, D.: Improvements in the Canadian Earth System Model (CanESM) through systematic model analysis: CanESM5.0 and CanESM5.1, Geoscientific Model Development, 16, 6553–6591, https://doi.org/10.5194/gmd-16-6553-2023, 2023.

Swart, N. C., Cole, J. N. S., Kharin, V. V., Lazare, M., Scinocca, J. F., Gillett, N. P., Anstey, J., Arora, V., Christian, J. R., Hanna, S., Jiao, Y., Lee, W. G., Majaess, F., Saenko, O. A., Seiler, C., Seinen, C., Shao, A., Sigmond, M., Solheim, L., Salzen, K. V., Yang, D., and Winter, B.: The Canadian Earth System Model version 5 (CanESM5.0.3), Geoscientific Model Development, 12, 4823–4873, https://doi.org/10.5194/gmd-12-4823-2019, 2019.

Séférian, R., Nabat, P., Michou, M., Saint-Martin, D., Voldoire, A., Colin, J., Decharme, B., Delire, C., Berthet, S., Chevallier, M., Sénési, S., Franchisteguy, L., Vial, J., Mallet, M., Joetzjer, E., Geoffroy, O., Guérémy, J. F., Moine, M. P., Msadek, R., Ribes, A., Rocher, M., Roehrig, R., Salas-y Mélia, D., Sanchez, E., Terray, L., Valcke, S., Waldman, R., Aumont, O., Bopp, L., Deshayes, J., Éthé, C., and Madec, G.: Evaluation of CNRM Earth System Model, CNRM-ESM2-1: Role of Earth System Processes in Present-Day and Future Climate, Journal of Advances in Modeling Earth Systems, 11, 4182–4227, https://doi.org/10.1029/2019MS001791, 2019.

Takemura, T., Egashira, M., Matsuzawa, K., Ichijo, H., O'Ishi, R., and Abe-Ouchi, A.: A simulation of the global distribution and radiative forcing of soil dust aerosols at the Last Glacial Maximum, Atmospheric Chemistry and Physics, 9, 3061–3073, https://doi.org/10.5194/acp-9-3061-2009, 2009.

Tatebe, H., Ogura, T., Nitta, T., Komuro, Y., Ogochi, K., Takemura, T., Sudo, K., Sekiguchi, M., Abe, M., Saito, F., Chikira, M., Watanabe, S., Mori, M., Hirota, N., Kawatani, Y., Mochizuki, T., Yoshimura, K., Takata, K., O'Ishi, R., Yamazaki, D., Suzuki, T., Kurogi, M., Kataoka, T., Watanabe, M., and Kimoto, M.: Description and basic evaluation of simulated mean state, internal variability, and climate sensitivity in MIROC6, Geoscientific Model Development, 12, 2727–2765, https://doi.org/10.5194/gmd-12-2727-2019, 2019.

Tegen, I., Harrison, S. P., Kohfeld, K., Prentice, I. C., Coe, M., and Heimann, M.: Impact of vegetation and preferential source areas on global dust aerosol: Results from a model study, Journal of Geophysical Research Atmospheres, 107, https://doi.org/10.1029/2001JD000963, 2002.

Tegen, I., Neubauer, D., Ferrachat, S., Drian, C. S. L., Bey, I., Schutgens, N., Stier, P., Watson-Parris, D., Stanelle, T., Schmidt, H., Rast, S., Kokkola, H., Schultz, M., Schroeder, S., Daskalakis, N., Barthel, S., Heinold, B., and Lohmann, U.: The global aerosol-climate model echam6.3-ham2.3 -Part 1: Aerosol evaluation, Geoscientific Model Development, 12, 1643–1677, https://doi.org/10.5194/gmd-12-1643-2019, 2019.

Textor, C., Schulz, M., Guibert, S., Kinne, S., Balkanski, Y., Bauer, S., Berntsen, T., Berglen, T., Boucher, O., Chin, M., Dentener, F., Diehl, T., Easter, R., Feichter, H., Fillmore, D., Ghan, S., Ginoux, P., Gong, S., Grini, A., Hendricks, J., Horowitz, L., Huang, P., Isaksen, I., Iversen, T., Kloster, S., Koch, D., Kirkevåg, A., Kristjansson, J. E., Krol, M., Lauer, A., Lamarque, J. F., Liu, X., Montanaro, V., Myhre, G., Penner, J., Pitari, G., Reddy, S., Seland, Stier, P., Takemura, T., and Tie, X.: Analysis and quantification of the diversities of aerosol life cycles within AeroCom, Atmospheric Chemistry and Physics, 6, 1777–1813, https://doi.org/10.5194/acp-6-1777-2006, 2006.

Volodin, E. M.: Possible Climate Change in Russia in the 21st Century Based on the INM-CM5-0 Climate Model, Russian Meteorology and Hydrology, 47, 327–333, https://doi.org/10.3103/S1068373922050016, 2022.

Volodin, E. M. and Kostrykin, S. V.: The aerosol module in the INM RAS climate model, Russian Meteorology and Hydrology, 41, 519–528, https://doi.org/10.3103/S106837391608001X, 2016.

Voss, K. K. and Evan, A. T.: A new satellite-based global climatology of dust aerosol optical depth, Journal of Applied Meteorology and Climatology, 59, 83–102, https://doi.org/10.1175/JAMC-D-19-0194.1, 2020.

White, B. R.: Soil transport by winds on Mars, Journal of Geophysical Research: Solid Earth, 84, 4643–4651, https://doi.org/10.1029/JB084iB09p04643, 1979.

Woodward, S.: Modeling the atmospheric life cycle and radiative impact of mineral dust in the Hadley Centre climate model, Journal of Geophysical Research Atmospheres, 106, 18 155–18 166, https://doi.org/10.1029/2000JD900795, 2001.

Woodward, S.: Hadley Centre Technical Note 87 - Mineral dust in HadGEM2, Tech. rep., Met Office, backup Publisher: Met Office, 2011.

Woodward, S., Sellar, A. A., Tang, Y., Stringer, M., Yool, A., Robertson, E., and Wiltshire, A.: The simulation of mineral dust in the United Kingdom Earth System Model UKESM1, Atmospheric Chemistry and Physics, 22, 14 503–14 528, https://doi.org/10.5194/acp-22-14503-2022, 2022.

Wu, C., Lin, Z., and Liu, X.: The global dust cycle and uncertainty in CMIP5 (Coupled Model Intercomparison Project phase 5) models, Atmospheric Chemistry and Physics, 20, 10 401–10 425, https://doi.org/10.5194/acp-20-10401-2020, 2020.

Xi, X. and Sokolik, I. N.: Dust interannual variability and trend in Central Asia from 2000 to 2014 and their climatic linkages, Journal of Geophysical Research: Atmospheres, 120, 12 175–12 197, https://doi.org/10.1002/2015JD024092, 2015a.

Xi, X. and Sokolik, I. N.: Seasonal dynamics of threshold friction velocity and dust emission in Central Asia, Journal of Geophysical Research: Atmospheres, 120, 1536–1564, https://doi.org/10.1002/2014JD022471, 2015b.

Xie, S., Terai, C., Wang, H., Tang, Q., Fan, J., Burrows, S., Lin, W., Wu, M., Song, X., Zhang, Y., Taylor, M., Golaz, J.-C., Benedict, J., Chen, C.-C., Feng, Y., Hannah, W., Ke, Z., Shan, Y., Larson, V., and Bader, D.: The Energy Exascale Earth System Model Version 3. Part I: Overview of the Atmospheric Component, Under Review, https://doi.org/10.22541/essoar.174456922.21825772/v1, 2025.

Yukimoto, S., Kawai, H., Koshiro, T., Oshima, N., Yoshida, K., Urakawa, S., Tsujino, H., Deushi, M., Tanaka, T., Hosaka, M., Yabu, S., Yoshimura, H., Shindo, E., Mizuta, R., Obata, A., Adachi, Y., and Ishii, M.: The meteorological research institute Earth system model version 2.0, MRI-ESM2.0: Description and basic evaluation of the physical component, Journal of the Meteorological Society of Japan, 97, 931–965, https://doi.org/10.2151/jmsj.2019-051, 2019.

Yumimoto, K., Tanaka, T. Y., Oshima, N., and Maki, T.: JRAero: The Japanese Reanalysis for Aerosol v1.0, Geoscientific Model Development, 10, 3225–3253, https://doi.org/10.5194/gmd-10-3225-2017, iSBN: 1991-9603 Publisher: Copernicus Publications, 2017.

Zender, C. S. and Kwon, E. Y.: Regional contrasts in dust emission responses to climate, Journal of Geophysical Research Atmospheres, 110, https://doi.org/10.1029/2004JD005501, 2005.

Zender, C. S., Bian, H., and Newman, D.: Mineral Dust Entrainment and Deposition (DEAD) model: Description and 1990s dust climatology, Journal of Geophysical Research: Atmospheres, 108, https://doi.org/10.1029/2002jd002775, 2003.

Zhao, A., Ryder, C. L., and Wilcox, L. J.: How well do the CMIP6 models simulate dust aerosols?, Atmospheric Chemistry and Physics, 22, 2095–2119, https://doi.org/10.5194/acp-22-2095-2022, 2022.

Zomer, R. J., Xu, J., and Trabucco, A.: Version 3 of the Global Aridity Index and Potential Evapotranspiration Database, Scientific Data, 9, https://doi.org/10.1038/s41597-022-01493-1, 2022.

Zou, X. K. and Zhai, P. M.: Relationship between vegetation coverage and spring dust storms over northern China, Journal of Geophysical Research: Atmospheres, 109, https://doi.org/10.1029/2003jd003913, 2004.